

Odd Yao-Yao Graphs are Not Spanners

Yifei Jin

Tsinghua University, China
jin-yf13@mails.tsinghua.edu.cn

Jian Li

Tsinghua University, China
lijian83@mail.tsinghua.edu.cn

Wei Zhan

Princeton University, USA
weizhan@cs.princeton.edu

Abstract

It is a long standing open problem whether Yao-Yao graphs YY_k are all spanners [26]. Bauer and Damian [4] showed that all YY_{6k} for $k \geq 6$ are spanners. Li and Zhan [23] generalized their result and proved that all even Yao-Yao graphs YY_{2k} are spanners (for $k \geq 42$). However, their technique cannot be extended to odd Yao-Yao graphs, and whether they are spanners are still elusive. In this paper, we show that, surprisingly, for any integer $k \geq 1$, there exist odd Yao-Yao graph YY_{2k+1} instances, which are not spanners.

1 Introduction

Let \mathcal{P} be a set of points in the Euclidean plane \mathbb{R}^2 . The complete Euclidean graph defined on set \mathcal{P} is the edge-weighted graph with vertex set \mathcal{P} and edges connecting all pairs of points in \mathcal{P} , where the weight of each edge is the Euclidean distance between its two end points. Storing the complete graph requires quadratic space, which is very expensive. Hence, it is desirable to use a sparse subgraph to approximate the complete graph. This is a classical and well-studied topic in computational geometry (see e.g., [1, 19, 26, 32, 34]). In this paper, we study the so called *geometric t -spanner*, formally defined as follows (see e.g., [29]).

Definition 1. (Geometric t -Spanner) A graph G is a *geometric t -spanner* of the complete Euclidean graph if (1) G is a subgraph of the complete Euclidean graph; and (2) for any pair of points p and q in \mathcal{P} , the shortest path between p and q in G is no longer than t times the Euclidean distance between p and q .

The factor t is called the *stretch factor* or *dilation factor* of the spanner in the literature. If the maximum degree of G is bounded by a constant k , we say that G is a *bounded-degree spanner*. The concept of geometric spanners was first proposed by L.P. Chew [10]. See the comprehensive survey by Eppstein [16] for related topics about geometric spanners. Geometric spanners have found numerous applications in wireless ad hoc and sensor networks. We refer the readers to the books by Li [24] and Narasimhan and Smid [27] for more details.

Yao graphs are one of the first approximations of complete Euclidean graphs, introduced independently by Flinchbaugh and Jones [18] and Yao [34].

Definition 2 (Yao Graph Y_k). Let k be a fixed integer. Given a set of points \mathcal{P} in the Euclidean plane \mathbb{R}^2 , the Yao graph $Y_k(\mathcal{P})$ is defined as follows. Let $C_u(\gamma_1, \gamma_2]$ be the cone with apex u , which consists of the rays with polar angles in the half-open interval $(\gamma_1, \gamma_2]$. For each point $u \in \mathcal{P}$, $Y_k(\mathcal{P})$ contains an edge connecting u to a nearest neighbor v in each cone $C_u(j\theta, (j+1)\theta]$, for $\theta = 2\pi/k$ and $j \in [0, k-1]$. We generally consider Yao graphs as undirected graphs. For a *directed Yao graph*, we add directed edge \vec{uv} to the graph instead.

Molla [15] showed that Y_2 and Y_3 may not be spanners. On the other hand, it has been proven that all Y_k for $k \geq 4$ are spanners. Bose et al. [6] proved that Y_4 is a 663-spanner. Damian and Nelavalli [13] improved this to 54.6 recently. Barba et al. [2] showed that Y_5 is a 3.74-spanner. Damian and Raudonis [14] proved that the Y_6 graph is a 17.64 spanner. Li et al. [25, 26] first proved that all $Y_k, k > 6$ are spanners with stretch factor at most $1/(1 - 2\sin(\pi/k))$. Later Bose et al. [6, 7] also obtained the same result independently. Recently, Barba et al. [2] reduced the stretch factor of Y_6 from 17.6 to 5.8 and improved the stretch factors to $1/(1 - 2\sin(3\pi/4k))$ for odd $k \geq 7$.

However, a Yao graph may not have bounded degree. This can be a serious limitation in certain wireless network applications since each node has very limited energy and communication capacity, and can only communicate with a small number of neighbors. To address the issue, Li et al. [26] introduced *Yao-Yao* graphs (or *Sparse-Yao* graphs in the literature). A Yao-Yao graph $YY_k(\mathcal{P})$ is obtained by removing some edges from $Y_k(\mathcal{P})$ as follows:

Definition 3 (Yao-Yao Graph YY_k). (1) Construct the directed Yao graph, as in Definition 2. (2) For each node u and each cone rooted at u containing two or more incoming edges, retain a shortest incoming edge and discard the other incoming edges in the cone. We can see that the maximum degree in $YY_k(\mathcal{P})$ is upper-bounded by $2k$.

As opposed to Yao graphs, the spanning property of Yao-Yao graphs is not well understood yet. Li et al. [26] provided some empirical evidence, suggesting that YY_k graphs are t -spanners for some sufficiently large constant k . However, there is no theoretical proof yet, and it is still an open problem [4, 23, 24, 26]. It is also listed as Problem 70 in the Open Problems Project.¹

Conjecture 1 (see [4]). There exists a constant k_0 such that for any integer $k > k_0$, any Yao-Yao graph YY_k is a geometric spanner.

Now, we briefly review the previous results about Yao-Yao graphs. It is known that YY_2 and YY_3 may not be spanners since Y_2 and Y_3 may not be spanners [15]. Damian and Molla [12, 15] proved that YY_4, YY_6 may not be spanners. Bauer et al. [2] proved that YY_5 may not be spanners. On the positive side, Bauer and Damian [4] showed that for any integer $k \geq 6$, any Yao-Yao graph YY_{6k} is a spanner with the stretch factor at most 11.67 and the factor becomes 4.75 for $k \geq 8$. Recently, Li and Zhan [23] proved that for any integer $k \geq 42$, any even Yao-Yao graph YY_{2k} is a spanner with the stretch factor $6.03 + O(k^{-1})$.

From these positive results, it is quite tempting to believe Conjecture 1. However, we show in this paper that, surprisingly, Conjecture 1 is false for odd Yao-Yao graphs.

Theorem 4. For any $k \geq 1$, there exists a class of point set instances $\{\mathcal{P}_m\}_{m \in \mathbb{Z}^+}$ such that the stretch factor of $YY_{2k+1}(\mathcal{P}_m)$ cannot be bounded by any constant, as m approaches infinity.²

¹<http://cs.smith.edu/~orourke/TOPP/P70.html>

²Here, m is a parameter in our recursive construction. We will explain it in detail in Section 3. Roughly speaking, m is the level of recursion and the number of points in \mathcal{P}_m increases with m .

Related Work It has been proven that in some special cases, Yao-Yao graphs are spanners [11, 21, 22, 33]. Specifically, it was shown that YY_k graphs are spanners in *civilized graphs*, where the ratio of the maximum edge length to the minimum edge length is bounded by a constant [21, 22].

Besides the Yao and Yao-Yao graph, the Θ -graph is another common geometric t -spanner. The difference between Θ -graphs and Yao graphs is that in a Θ -graph, the nearest neighbor to u in a cone C is a point $v \neq u$ lying in C and minimizing the Euclidean distance between u and the orthogonal projection of v onto the bisector of C . It is known that except for Θ_2 and Θ_3 [15], for $k = 4$ [3], 5 [8], 6 [5], ≥ 7 [9, 28], Θ_k -graphs are all geometric spanners. We note that, unfortunately, the degrees of Θ -graphs may not be bounded.

Recently, some variants of geometric t -spanners such as weak t -spanners and power t -spanners have been studied. In weak t -spanners, the path between two points may be arbitrarily long, but must remain within a disk of radius t -times the Euclidean distance between the points. It is known that all Yao-Yao graphs YY_k for $k > 6$ are weak t -spanners [20, 30, 31]. In power t -spanners, the Euclidean distance $|\cdot|$ is replaced by $|\cdot|^\kappa$ with a constant $\kappa \geq 2$. Schindelhauer et al. [30, 31] proved that for $k > 6$, all Yao-Yao graphs YY_k are power t -spanners for some constant t . Moreover, it is known that any t -spanner is also a weak t_1 -spanner and a power t_2 -spanner for some t_1, t_2 depending only on t . However, the converse is not true [31].

Our counterexample is inspired by the concept of fractals. Fractals have been used to construct examples for β -skeleton graphs with unbounded stretch factors [17]. Here a β -skeleton graph is defined to contain exactly those edges ab such that no point c forms an angle $\angle acb$ greater than $\sin^{-1} 1/\beta$ if $\beta > 1$ or $\pi - \sin^{-1} \beta$ if $\beta < 1$. Schindelhauer et al. [31] used the same example to prove that there exist graphs which are weak spanners but not t -spanners. However, their examples cannot serve as counterexamples to the conjecture that odd Yao-Yao graphs are spanners.

2 Overview of our Counterexample Construction

We first note that both the counterexamples for YY_3 and YY_5 are not weak t -spanners [2, 15]. However, Yao-Yao graphs YY_k for $k \geq 7$ are all weak t -spanners [20, 30, 31]. Hence, to construct the counterexamples for YY_k for $k \geq 7$, the previous ideas for YY_3 and YY_5 cannot be used. We will construct a class of instances $\{\mathcal{P}_m\}_{m \in \mathbb{Z}^+}$ such that all points in \mathcal{P}_m are placed in a bounded area. Meanwhile, there exist shortest paths in $YY_{2k+1}(\mathcal{P}_m)$ whose lengths approach infinity as m approaches infinity.

Our example contains two types of points, called *normal points* and *auxiliary points*. Denote them by \mathcal{P}_m^n and \mathcal{P}_m^a respectively and $\mathcal{P}_m = \mathcal{P}_m^n \cup \mathcal{P}_m^a$. The normal points form the basic skeleton, and the auxiliary points are used to break the edges connecting any two normal points that are far apart.

We are inspired by the concept of fractals to construct the normal points. A fractal can be contained in a bounded area, but its length may diverge. In our counterexample, the shortest path between two specific normal points is a fractal-like polygonal path. Here a polygonal path refers to a curve specified by a sequence of points and consists of the line segments connecting the consecutive points. Suppose the two specific points are A and B , AB is horizontal, and $|AB| = 1$. When $m = 0$, the polygonal path is just the line segment AB . When m increases by one, we replace each line segment in the current polygonal path by a *sawteeth-like* path (see Figure 1a). If the angle between each segment of the sawteeth-like path and the base segment (i.e., the one

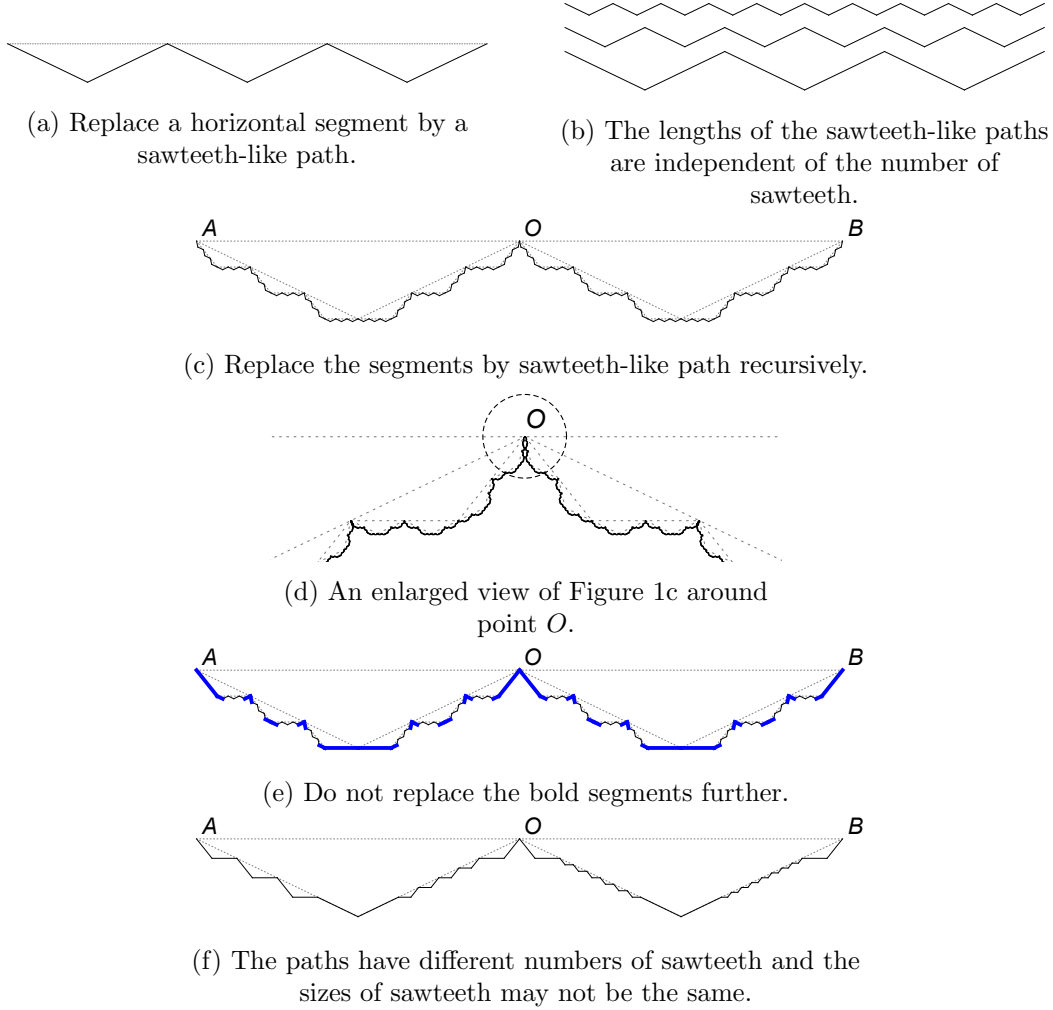


Figure 1: The overview of the counterexample construction. Figure 1a-1f illustrate the fractal and its variants.

which is replaced) is γ , the total length of the path increases by a factor of $\cos^{-1} \gamma$. An important observation here is that the factor is independent of the number of sawteeth (see Figure 1b). If we repeat this process directly, the length of the resulting path would increase to infinity as m approaches infinity since $\cos^{-1} \gamma > 1$ (see Figure 1c). However, we need to make sure that such a path is indeed in a Yao-Yao graph and it is indeed the shortest path from A to B . There are two technical difficulties we need to overcome.

1. As m increases, the polygonal path may intersect itself. See Figure 1d. The polygonal path intersects itself around the point O . This is relatively easy to handle: we do not recurse for those segments that may cause self-intersection. See Figure 1e. We do not replace the bold segment further. We need to make sure that the total length of such segments is proportionally small (so that the total length can keep increasing as m increases).
2. In the Yao-Yao graph defined over the normal points constructed in the recursion, there may

be some edges connecting points that are far apart. Actually, how to break such edges is the main difficulty of the problem. We outline the main techniques below.

First, we *do not* replace all current segments using the same sawteeth, like in the usual fractal construction. Actually, for each segment, we will choose a polygonal path such that the paths have different numbers of sawteeth and the sizes of the sawteeth in the path may not be the same. See Figure 1f. Finally, we construct them in a specific sequential order. Actually, we organize the normal points in an m -level *recursion tree* \mathcal{T} and generate them in a DFS preorder traversal of the tree. We describe the details in Section 3.

Second, we group the normal points into a collection of sets such that each normal point belongs to exactly one set. We call such a set a *hinge set*. Refer to Figure 13 for an overview. Then, we specify a *total order* of the hinge sets. Call the edges in the Yao-Yao graph $\mathbb{Y}\mathbb{Y}_{2k+1}(\mathcal{P}_m^n)$ connecting any two normal points in the same hinge set or two adjacent hinge sets (w.r.t. the total order) *hinge connections* and call the other edges *long range connections*. We describe the details in Section 4.

As we will see, all possible long range connections have a relatively simple form. Then, we show that we can break all long range connections by adding a set \mathcal{P}_m^a of *auxiliary points*. Each auxiliary point has a unique *center* which is the normal point closest to it. Let the minimum distance between any two normal points in \mathcal{P}_m^n be Δ . The distance between an auxiliary point and its center is much less than Δ . Naturally, we can extend the concepts of hinge set and long range connection to include the auxiliary points. An *extended hinge set* consists of the normal points in a hinge set and the auxiliary points centered on these normal points. We will see that the auxiliary points break all long range connections and introduce no new long range connection. We describe the details in Section 5.

Finally, according to the process above, we can see that the shortest path between the normal points A and B in $\mathbb{Y}\mathbb{Y}_{2k+1}(\mathcal{P}_m)$ for $m \in \mathbb{Z}^+$ should pass through all extended hinge sets in order. Thereby, the length of the shortest path between A and B diverges as m approaches infinity. We describe the details in Section 6.

3 The Positions of Normal Points

In this section, we describe the positions of normal points. Note that, in the section, we only care about the positions of the points. The segments in any figure of this section are used to illustrate the relative positions of the points. Those segments may not represent the edges in Yao or Yao-Yao graphs. See Figure 2 for an overview of the positions of the normal points.

3.1 Some Basic Concepts

Let $k \geq 3$ be a fixed positive integer.³ We consider $\mathbb{Y}\mathbb{Y}_{2k+1}$ and let $\theta = 2\pi/(2k+1)$.

Definition 5 (Cone Boundary). Consider any two points u and v . If the polar angle of \vec{uv} is $j\theta = j \cdot 2\pi/(2k+1)$ for some integer $j \in [0, 2k]$, we call the ray \vec{uv} a cone boundary for point u .

Note that in an odd Yao-Yao graph, if \vec{uv} is a cone boundary, its reverse \vec{vu} is not a cone boundary. In retrospect, this property is a key difference between odd Yao-Yao graphs and even Yao-Yao graphs, and our counterexample for odd Yao-Yao graphs will make crucial use of the property. We make it explicit as follows.

³Note that the cases $k = 1, 2$ have been proved in [15].

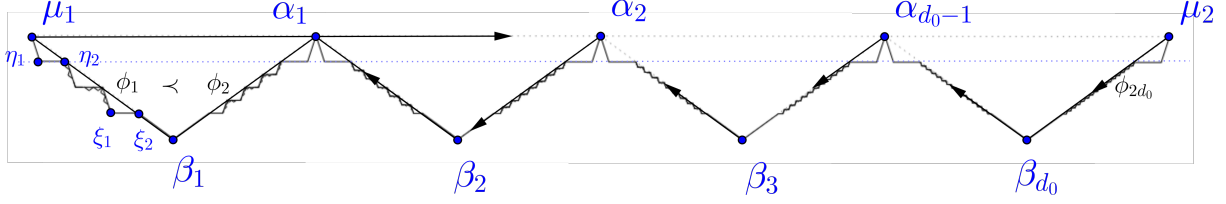


Figure 2: The overview of the positions of normal points. There exists a point at each intersection of these segments. $\mu_1\mu_2$ is horizontal. $\{\alpha_1, \alpha_2, \dots, \alpha_{d_0-1}\}$ partitions the segment $\mu_1\mu_2$ into d_0 equal parts. For each β_i , $\angle\alpha_{i-1}\beta_i\alpha_i = \pi - \theta$ and $|\alpha_{i-1}\beta_i| = |\beta_i\alpha_i|$. We call $\{\alpha_1, \alpha_2, \dots, \alpha_{d_0-1}\}$ the partition set and $\{\beta_1, \beta_2, \dots, \beta_{d_0}\}$ the apex set of pair (μ_1, μ_2) .

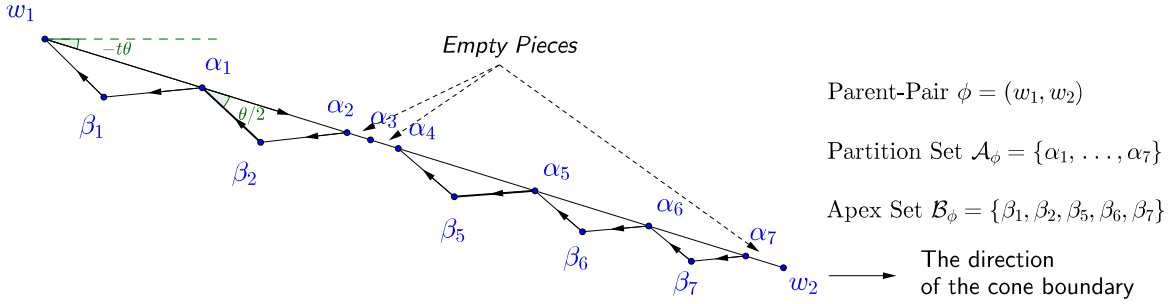


Figure 3: An example of one gadget. $\phi = (w_1, w_2)$ is the parent-pair in the gadget. $\mathcal{A}_\phi = \{\alpha_1, \alpha_2, \alpha_3, \dots, \alpha_7\}$ is the partition set and $\mathcal{B}_\phi = \{\beta_1, \beta_2, \beta_5, \beta_6, \beta_7\}$ is the apex set. There are eight pieces, in which $w_1\alpha_1, \alpha_1\alpha_2, \alpha_4\alpha_5, \alpha_5\alpha_6, \alpha_6\alpha_7$ are non-empty pieces and $\alpha_2\alpha_3, \alpha_3\alpha_4, \alpha_7w_2$ are empty pieces.

Property 6. Consider two points u and v in \mathcal{P} . If \overrightarrow{uv} is a cone boundary in $\mathbb{Y}_{2k+1}(\mathcal{P})$, its reverse \overrightarrow{vu} is not a cone boundary.

Definition 7 (Boundary Pair). A boundary pair consists of two ordered points, denoted by (w_1, w_2) , such that $\overrightarrow{w_1w_2}$ is a cone boundary of point w_1 .

For convenience, we refer to the word *pair* in the paper as the boundary pair defined in Definition 7. According to Property 6, if (w_1, w_2) is a pair, its reverse (w_2, w_1) is not a pair. For a pair $\phi = (w_1, w_2)$, we call w_1 the first point in ϕ and w_2 the second point in ϕ . Moreover, if a pair ϕ is (u, \cdot) or (\cdot, u) , we say that the point u belongs to ϕ (i.e., $u \in \phi$).

Gadget: Now, we introduce the concept of a gadget generated by a pair $\phi = (w_1, w_2)$. Such a gadget is a collection of points which is a superset of ϕ (see Figure 3). If the recursive level m increases by 1, we use a gadget generated by pair ϕ to replace ϕ .

One gadget G_ϕ consists of three groups of points. We explain them one by one. See Figure 3 for an example.

1. The first group is the pair $\phi = (w_1, w_2)$. We call the pair the *parent-pair* of the gadget G_ϕ .
2. The second group is a set \mathcal{A}_ϕ of points on the segment of (w_1, w_2) . We call the set \mathcal{A}_ϕ a *partition set* and call the points of \mathcal{A}_ϕ the *partition points* of ϕ . For example, in Figure 3,

$\{\alpha_1, \alpha_2, \dots, \alpha_7\}$ (here, $|w_1\alpha_i| < |w_1\alpha_j|$ if $i < j$) is a partition set of (w_1, w_2) . The set \mathcal{A}_ϕ divides the segment into $|\mathcal{A}_\phi| + 1$ parts, each we call a *piece* of the segment. There are two types of pieces. One is called an *empty piece* and the other a *non-empty piece*. Whether a piece is empty or not is determined in the process of the construction, which we will explain in Section 3.3.

3. For each non-empty piece, $\alpha_{i-1}\alpha_i$, we add a point β_i such that $\angle\alpha_{i-1}\beta_i\alpha_i = \pi - \theta$ and $|\alpha_{i-1}\beta_i| = |\beta_i\alpha_i|$.⁴ All β_i s are on the same side of w_1w_2 . We call such a point β_i an *apex point* of (w_1, w_2) . Let \mathcal{B}_ϕ be the set of apex points generated by ϕ , which is called the *apex set* of pair ϕ . \mathcal{B}_ϕ is the third group of points. For any empty piece, we do not add the corresponding apex point. In Figure 3, $\{\beta_1, \beta_2, \beta_5, \beta_6, \beta_7\}$ is an apex set of (w_1, w_2) .

We summarize the above construction in the following definition.

Definition 8 (Gadget). A gadget G_ϕ generated by a pair ϕ is a set of points which consists of the pair ϕ , a partition set \mathcal{A}_ϕ and an apex set \mathcal{B}_ϕ of ϕ . We denote the gadget by $G_\phi[\mathcal{A}_\phi, \mathcal{B}_\phi]$.

Consider a gadget $G_\phi[\mathcal{A}_\phi, \mathcal{B}_\phi]$, where $\phi = (w_1, w_2)$. For any non-empty piece $\alpha_{i-1}\alpha_i$ and the corresponding apex point β_i , the rays $\overrightarrow{\beta_i\alpha_{i-1}}$ and $\overrightarrow{\alpha_i\beta_i}$ (note the order of the points) are cone boundaries.⁵ Thus, each point $\beta_i \in \mathcal{B}_\phi$ induces two pairs (β_i, α_{i-1}) and (α_i, β_i) . We call all pairs (β_i, α_{i-1}) and (α_i, β_i) induced by points in \mathcal{B}_ϕ the *child-pairs* of (w_1, w_2) , and we say that they are *siblings* of each other. Now, we define the order of the child-pairs of pair (w_1, w_2) , based on their distances to w_1 . Here, the distance from a point w to a pair ϕ is the shortest distance from w to any point of ϕ .

Definition 9 (The Order of the Child-pairs). Consider a gadget $G_{(w_1, w_2)}$. Suppose Φ is the set of the child-pairs of (w_1, w_2) . Consider two pairs ϕ, φ in Φ . Define the order $\phi \prec \varphi$, if ϕ is closer to w_1 than φ .

For example, in Figure 3, $(\beta_2, \alpha_1) \prec (\alpha_5, \beta_5)$. We emphasize that the order of the child-pairs depends on the direction of their parent-pair.

3.2 The Recursion Tree

In this subsection, we construct an m -level tree. When the recursion level increases by 1, we need to replace each current pair by a gadget generated by the pair. The recursion can be naturally represented as a tree \mathcal{T} . Each node of the tree represents either a pair or a point. To avoid confusion, we use *point* to express a point in \mathbb{R}^2 and *node* to express a vertex in the tree. The pair (μ_1, μ_2) is the root of the tree (*level-0*). The child-pairs of (μ_1, μ_2) are the child-nodes of the root (they are at *level-1*). Recursively, each child-pair of a pair ϕ is a child-node of the node ϕ in \mathcal{T} . Besides, there are some *partition points* of the empty pieces (e.g., the point α_3 in Figure 4) which may not belong to any pair. We call it an *isolated point*. Let an isolated point be a leaf in \mathcal{T} and the parent of such a point be its parent pair. For example, the parent of α_3 is the pair (ω_1, ω_2) in Figure 4. We provide the recursion tree in Figure 5, which corresponds to the points in Figure 4.

⁴Note that the subscript i of β_i is consistent with the subscript of the piece $\alpha_{i-1}\alpha_i$. Hence, the subscripts may not be consecutive among all β_i s.

⁵ Suppose the polar angle of w_1w_2 is $-t\theta$. Note that $(2k+1)\theta = 2\pi$. Then, we can obtain that the polar angle of $\overrightarrow{\alpha_i\beta_i}$ is $(k-t+1)\theta$ and the polar angle of $\overrightarrow{\beta_i\alpha_{i-1}}$ is $(k-t)\theta$. Hence, $\overrightarrow{\alpha_i\beta_i}$ and $\overrightarrow{\beta_i\alpha_{i-1}}$ are cone boundaries.

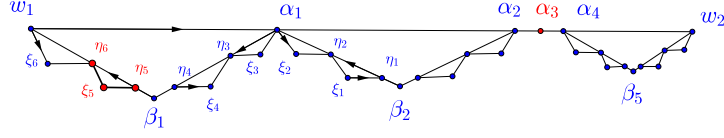


Figure 4: An example of the gadgets which are generated in a recursive manner. α_3 is an isolated partition point. The arrow of a segment indicates the order of two points in the pair. For example, the arrow from w_1 to w_2 indicates that (w_1, w_2) is a pair.

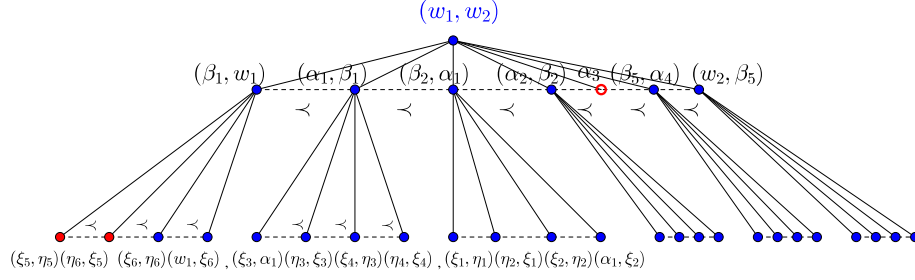


Figure 5: The recursion tree of our construction. Each node of the tree represents a pair (e.g., (β_1, w_1)) or a point (e.g., α_3) in Figure 4. Pair (w_1, w_2) is the root at *level-0*. Any pair at *level-(i + 1)* is generated from a pair at *level-i*.

The nodes with the same parent are siblings. According to Definition 9, we define a total order “ \prec ” of them. In tree \mathcal{T} , if “ $\varphi \prec \phi$ ”, we place φ to the left of ϕ , (e.g., (ξ_5, η_5) is at the left of (η_6, ξ_5) in Figure 5). However, “ $\varphi \prec \phi$ ” does not mean that φ is on the left hand side of ϕ geometrically. For example, in Figure 4, pair $(\xi_5, \eta_5) \prec (\eta_6, \xi_5)$ in the tree \mathcal{T} , but in the Euclidean plane, point η_5 is on the right side of η_6 .

For a pair ϕ (corresponding to a node in \mathcal{T}), we use \mathcal{T}_ϕ to denote the subtree rooted at ϕ (including ϕ), or all the points involved in the subtree.

Our counterexample \mathcal{P}_m corresponds to a recursion tree with m levels. We have not yet specified how to choose the partition set for each gadget and decide which pieces are empty for each pair. We will do it in the next subsection. We note that we *do not* construct the tree level by level, but rather according to the DFS preorder.

3.3 The Construction

Now, we describe the process of generating the m -level recursion tree \mathcal{T} . See Figure 6 for an example. We call a pair a *leaf-pair* if it is a leaf node in the tree and an *internal-pair* otherwise. W.l.o.g, we assume that the root of \mathcal{T} is (μ_1, μ_2) and $\mu_1\mu_2$ is horizontal. The tree is generated according to the DFS preorder, starting from the root. When we are visiting an internal-pair, we generate its gadget. Note that generating its gadget is equivalent to generating its children in \mathcal{T} . We, however, do not visit those children immediately after their generation. They will be visited later according to the DFS preorder. Whether a pair is a leaf or not is determined as the gadget being created. Note that not all leaf-pairs are at *level-m*.

The process generating the gadget for an internal-pair includes two steps, which are called

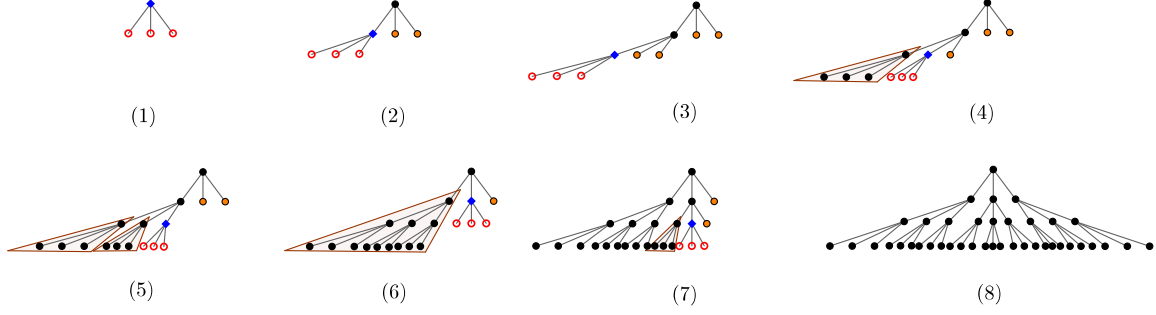


Figure 6: The process of generating a tree according to the DFS preorder. In each subfigure, \diamond represents a node we are visiting. The nodes generated in the step are denoted by \circ . \bullet represents a node which has already been visited. \circ represents a node which has been created but not visited yet. The nodes covered by light brown triangles are related to the projection process.

Algorithm 1: GenGadget(ϕ): Generate the Normal Points in \mathcal{T}_ϕ

```

1 if  $\phi$  is a leaf-pair then
2   | Return ;
3 else
4   |  $G_\phi \leftarrow \text{Proj-Refn}(\phi)$ ;
5 foreach child-pair  $\varphi$  of  $\phi$  do
6   | GenGadget( $\varphi$ ) ;
```

projection and *refinement*. We will explain the detail soon. We denote the procedure to construct the recursion tree \mathcal{T} by GenGadget(ϕ) and the pseudocode can be found in Algorithm 1. We call the points generated by Algorithm 1 *normal points* and denote them by \mathcal{P}_m^n where m is the level of the tree and n represents the word “normal”.

Root gadget: Let d_0 be a large positive constant integer.⁶ Consider a pair $\phi = (\mu_1, \mu_2)$. Let \mathcal{A}_ϕ be its partition set which contains points

$$\alpha_i = \mu_1 \cdot \frac{d_0 - i}{d_0} + \mu_2 \cdot \frac{i}{d_0}, i \in [1, d_0 - 1].$$

For convenience, let $\alpha_0 = \mu_1, \alpha_{d_0} = \mu_2$. The points in \mathcal{A}_ϕ partition the segment $\mu_1\mu_2$ into d_0 pieces with equal length $|\mu_1\mu_2|/d_0$. All pieces in the root gadget are non-empty. For each piece $\alpha_{i-1}\alpha_i$, we add an apex point β_i below $\mu_1\mu_2$. Let $\mathcal{B}_\phi = \{\beta_i\}_{i \in [1, d_0]}$ be the apex set. See Figure 7 for an example.

Projection and Refinement: Let \mathcal{T}_ϕ be the set of points in the subtree rooted at ϕ . The projection and refinement process for ϕ is slightly more complicated, as it depends on the subtrees \mathcal{T}_φ rooted at the siblings φ of ϕ such that $\varphi \prec \phi$. Recall that when we visit a pair ϕ (and generate G_ϕ) in the tree \mathcal{T} according to the DFS preorder, we have already visited all pairs $\varphi \prec \phi$.

⁶ d_0 depends on k , but on the number of points. We will determine the exact value of d_0 in Section 6.

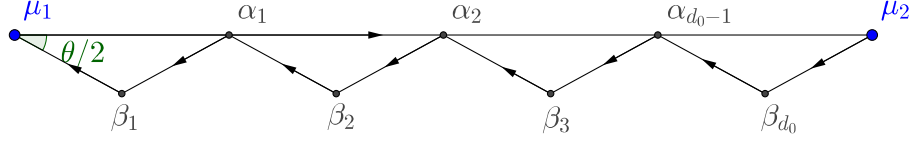


Figure 7: The root gadget $G_\phi(\mathcal{A}_\phi, \mathcal{B}_\phi)$ where $\phi = (\mu_1, \mu_2)$. $\mu_1\mu_2$ is horizontal. \mathcal{A}_ϕ is the equidistant partition. Each piece is non-empty.

The projection and refinement generate the partition points of pair ϕ . The purpose of the projection is to restrict all possible *long range connections* to a relatively simple form. See Section 4 for the details. The purpose of the refinement is to make the sibling pairs have relatively the same length, hence, make it possible to repeat the projection process recursively. Formally speaking, the refinement maintains the following property over the construction.

Property 10. We call the segment connecting the two points of the pair the *segment of the pair* and call the length of that segment the *length of the pair*. Consider an internal-pair ϕ . Suppose φ is a sibling of ϕ . The length of pair φ is at least half of the length of pair ϕ .

– **Projection:** Consider a pair (β, α) with the set Φ being its child-pairs. We decide whether a pair in Φ is a leaf-pair or an internal-pair after introducing the process projection and refinement. We provide that the property of the order here and prove it in the end of the section.

Property 11. Consider a pair (β, α) with the set Φ of its child-pairs. For $\phi_1, \phi_2, \phi_3 \in \Phi$, if $\phi_1 \prec \phi_2 \prec \phi_3$ and ϕ_1 and ϕ_3 are two internal-pairs, then ϕ_2 is an internal-pair.

Next, we describe the projection operation for a pair $\phi \in \Phi$. W.l.o.g., suppose ϕ is an internal-pair since only internal-pairs have children. We define the first internal-pair in direction $\overrightarrow{\beta\alpha}$ as the *first internal-pair* of Φ . Depending on whether ϕ is the first internal-pair of Φ , there are two cases.

- Pair ϕ is the first internal-pair of Φ : In Figure 8, suppose pair $\phi = (\eta, \xi)$ is the first internal child-pair of (β, α) and the length of ϕ is δ . Point ξ is the partition point in ϕ . First, we add a point λ on the segment of ϕ such that $|\xi\lambda| = \delta/d_0$. Second, for each leaf-pair $\varphi \prec \phi$, project the apex point in φ to the segment of ϕ along the direction $\overrightarrow{\beta\alpha}$,⁷ e.g., project p to q in Figure 8. Note that the length of leaf-pair φ is at least $\delta/2$ according to Property 10. Thus, there is no point between λ and ξ as long as $d_0 > 2$. Formally, we denote the operation by

$$\hat{\mathcal{A}}_\phi \leftarrow \text{Proj} \left[\bigcup_{\varphi \prec \phi, \varphi \in \Phi} \mathcal{T}_\varphi \right] \cup \lambda. \quad (1)$$

- Pair ϕ is not the first internal-pair: According to the DFS preorder, we have already constructed the subtrees rooted at $\varphi \prec \phi$. We project all points $p \in \bigcup_{\varphi \prec \phi, \varphi \in \Phi} \mathcal{T}_\varphi$, to the segment of ϕ along the direction $\overrightarrow{\beta\alpha}$. Let the partition set $\hat{\mathcal{A}}_\phi$ of ϕ be the set of the projected points

⁷If the projected point falls outside the segment of ϕ , we do not need to add a normal point.

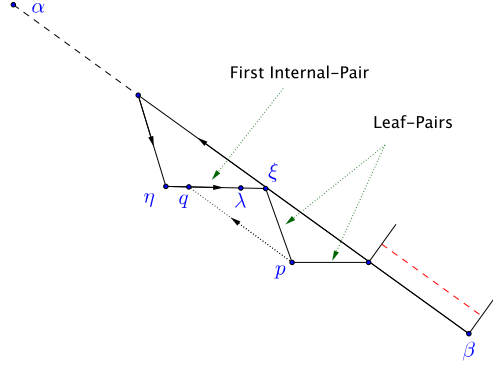


Figure 8: An example of the projection for the first internal-pair $\phi = (\eta, \xi)$. First, we add a point λ such that $|\lambda\xi| = \delta/d_0$ where δ is the length $|\eta\xi|$. Second, for each leaf-pair $\varphi \prec \phi$, project its apex point p to the segment of ϕ along the direction $\vec{\beta\alpha}$, i.e., add the point q in the figure.

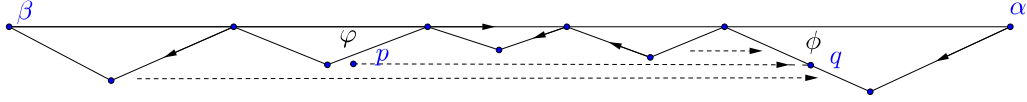


Figure 9: The projection for pair ϕ . Here, p is a point in subtree \mathcal{T}_φ . q is a projection point of p , i.e., the point on segment of pair ϕ such that pq is parallel to $\beta\alpha$. The set $\text{Proj}[\bigcup_{\varphi \prec \phi, \varphi \in \Phi} \mathcal{T}_\varphi]$ consists of all projection points of $\bigcup_{\varphi \prec \phi, \varphi \in \Phi} \mathcal{T}_\varphi$ on segment of ϕ .

falling inside the segment of ϕ . If several points overlap, we keep only one of them. See Figure 9 for an example. Formally, we denote the operation by

$$\hat{\mathcal{A}}_\phi \leftarrow \text{Proj} \left[\bigcup_{\varphi \prec \phi, \varphi \in \Phi} \mathcal{T}_\varphi \right]. \quad (2)$$

– **Refinement:** After the projection, we obtain a candidate partition set $\hat{\mathcal{A}}_\phi$ of ϕ (defined in (1) and (2)). However, note that the length between the pieces may differ a lot. In order to maintain Property 10, we add some other points to ensure that all non-empty pieces of ϕ have approximately the same length. We call this process the *refinement* operation.

W.l.o.g., suppose pair ϕ has unit length and $|\hat{\mathcal{A}}_\phi| = n$ and $n > d_0$.⁸

Suppose $\phi = (u_1, u_2)$. We distinguish into two cases based on whether the first point u_1 is a partition point or an apex point.

- If u_1 is an apex point, we mark the piece incident on u_2 . See Figure 10a for an illustration, in which $(u_1, u_2) = (\beta, \alpha_1)$ and piece $\alpha_1\eta_1$ is the marked piece.
- If u_1 is a partition point, we mark the pieces incident on u_1 and u_2 . See Figure 10b for an illustration, in which $(u_1, u_2) = (\alpha_2, \beta)$ and piece $\alpha_2\eta_2$ and $\xi_2\beta$ are the marked pieces.

⁸ If $n \leq d_0$, we repeatedly split the inner pieces (i.e., all pieces except for the two pieces incident on the points of ϕ) into two equal-length pieces until the number of the points in $\hat{\mathcal{A}}_\phi$ is larger than d_0 .

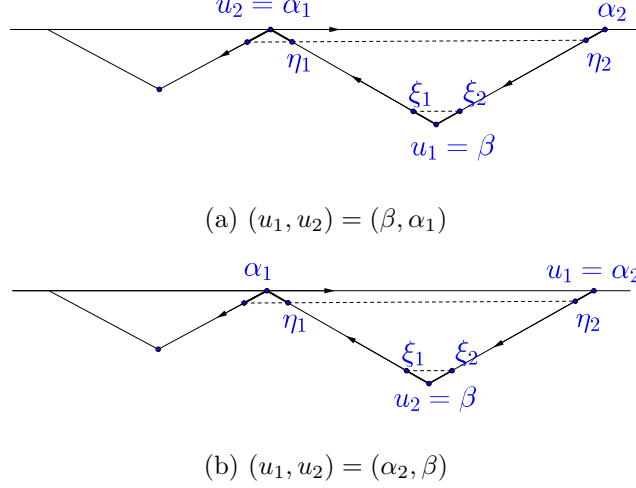


Figure 10: The two cases for refinement. The first case is $\phi = (\beta, \alpha_1)$ in which the first point is an apex point. We mark the piece incident on α_1 , i.e., the piece $\alpha_1\eta_1$. The second case is $\phi = (\alpha_2, \beta)$, in which the first point is a partition point. We mark the two pieces incident on α_2 and β respectively, i.e., the pieces $\alpha_2\eta_2$ and $\xi_2\beta$. Note that after refinement, $|\beta\xi_1| = |\beta\xi_2|$ and $|\alpha_1\eta_1| = |\alpha_2\eta_2|$ since there is no point added on the marked pieces after refinement.

We do not add any point in the marked pieces under refinement. Consider two sibling pairs (β, α_1) and (α_2, β) where β is an apex point. Suppose $\alpha_1\eta_1, \alpha_2\eta_2, \xi_2\beta$ are the marked pieces of the two pairs and ξ_1 is the point on the segment $\beta\alpha_1$ which is projected to ξ_2 .⁹ Then $|\beta\xi_1| = |\beta\xi_2|$ and $|\alpha_1\eta_1| = |\alpha_2\eta_2|$ after the refinement. See Figure 10 for an example.

Denote the length of the i th piece (defined by $\hat{\mathcal{A}}_\phi$) by δ_i . Let $\delta_o = 1/n^2$. Except for the marked pieces¹⁰, for each other piece which is at least twice longer than δ_o , we place $\lfloor \delta_i/\delta_o \rfloor - 1$ equidistant points on the piece, which divide the piece into $\lfloor \delta_i/\delta_o \rfloor$ equal-length parts.

We call this process the *refinement* and denote the resulting point set by

$$\mathcal{A}_\phi \leftarrow \text{Refine}[\hat{\mathcal{A}}_\phi]. \quad (3)$$

The number of points added in the refinement process is at most $O(n^2)$ since the segment of pair ϕ has unit length and $\delta_o \geq 1/n^2$. We call each piece whose length is less than δ_o a *short piece*. The short pieces remain unchanged before and after the refinement. Moreover, the refinement does not introduce any new short piece for the pair.

Deciding Emptiness, Leaf-Pairs and Internal-Pairs: Next, we discuss the principle to decide whether a piece is empty or non-empty. See Figure 11 for an illustration. Consider a pair ϕ whose apex point is β and partition point is α .¹¹ We let the piece incident on the apex point β and the short pieces be empty and the other pieces be non-empty.

⁹Point ξ_1 must exist since ξ_2 is a projected point and there is no point in the marked piece $\xi_2\beta$.

¹⁰Keeping the marked pieces unchanged maintains Property 12 and helps a lot to decompose the normal points into hinge sets. See Section 4 for details.

¹¹Note that the first point of a pair can be either apex point or partition point. Here, $\phi = (\alpha, \beta)$ or $\phi = (\beta, \alpha)$ depending on whether first point of ϕ is apex point or not.

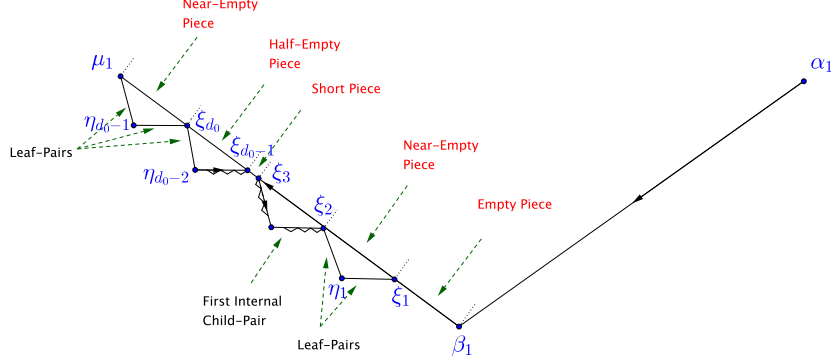


Figure 11: The figure illustrates the emptiness of each piece. Consider the pair (β_1, μ_1) with partition points after refinement. Segment $\mu_1\xi_{d_0}$ and $\xi_1\xi_2$ are two near-empty pieces and $\beta_1\xi_1$ is an empty piece. Pair (μ_1, η_{d_0-1}) and $(\eta_{d_0-1}, \xi_{d_0})$, $(\xi_{d_0}, \eta_{d_0-2})$, (ξ_2, η_1) , (η_1, ξ_1) are the five leaf-pairs. $\xi_{d_0-1}\xi_{d_0}$ is the half-empty piece. Pair (η_2, ξ_2) is the first internal-pair.

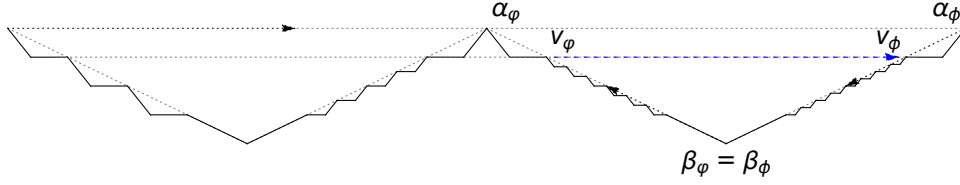


Figure 12: The figure illustrates Property 12. After projection and refinement, $|\alpha_\phi v_\phi| = |\alpha_\varphi v_\varphi|$.

For each non-empty piece, we generate one apex point. The apex set \mathcal{B}_ϕ induces the set Φ of child-pairs of ϕ . The types of these pairs are determined as follows. Let the three pairs closest to α and two pairs closest to β be *leaf-pairs*. We do not further expand the tree from the leaf-pairs. Let the other pairs be the *internal-pairs*. Naturally, there is no leaf-pair between any two internal-pairs among pairs in Φ . Hence, Property 11 maintains in the construction. Further, we can see that each other normal point belongs to at most two pairs, except for the two points in the root pair.

For convenience, we call the piece generating two leaf-pairs a *near-empty piece* and generating one leaf-pair and one internal-pair a *half-empty piece*. Note that the near-empty and half-empty pieces are special non-empty pieces. We can see that, except for the near-empty piece incident on the partition point in ϕ (e.g., $\mu_1\xi_{d_0}$ in Figure 11), the maximum length among the non-empty pieces is at most twice longer than the minimum one according to refinement.

Overall, after the projection and refinement process, we can generate the gadget for any pair in the tree. We denote this process by

$$\mathcal{G}_\phi \leftarrow \text{Proj-Refn}(\phi). \quad (4)$$

Property 12. Consider two sibling pairs ϕ and φ . Suppose both of them are internal-pairs and have partition point sets \mathcal{A}_ϕ and \mathcal{A}_φ respectively. Suppose $\alpha_\phi \in \phi$ and $\alpha_\varphi \in \varphi$, and both α_ϕ and α_φ are partition points. The point in \mathcal{A}_ϕ closest to α_ϕ is v_ϕ . Meanwhile, the point in \mathcal{A}_φ closest to α_φ is v_φ . Then $|\alpha_\phi v_\phi| = |\alpha_\varphi v_\varphi|$. See Figure 12 for an example.

Proof. W.l.o.g., we prove that any two adjacent siblings satisfy the property. Suppose ϕ and φ are adjacent siblings. W.l.o.g., assume $\varphi \prec \phi$. ϕ has the candidate partition set $\hat{\mathcal{A}}_\phi$ after projection. Suppose the point in $\hat{\mathcal{A}}_\phi$ closest to α_ϕ is \hat{v}_ϕ . According to the projection, we know $|\alpha_\phi \hat{v}_\phi| = |\alpha_\varphi v_\varphi|$. Since we do not add any new point between $\alpha_\phi \hat{v}_\phi$ after refinement, \hat{v}_ϕ and v_ϕ are the same point. Hence, any two adjacent siblings have the property. \square

Corollary 13. Consider a pair ϕ with partition point set \mathcal{A}_ϕ . Suppose $\alpha \in \phi$ and α is a partition point. Among all pieces determined by \mathcal{A}_ϕ , the piece incident on α has the maximum length.

Proof. It is not difficult to check the root pair holds the property. Then, consider a pair $\hat{\phi}$ with its child pair set $\hat{\Phi}$. We prove that any pair in $\hat{\Phi}$ holds the property when $\hat{\phi}$ holds the property. Suppose ϕ is the first internal-pair in $\hat{\Phi}$, the corollary is trivially true for ϕ according to the projection process (the first projection case). Otherwise, according to Property 12 and the projection process, we know that for any ϕ in $\hat{\Phi}$, the piece incident on the partition point in ϕ has the same length. Thus, any pair in $\hat{\Phi}$ holds the property. \square

Now, we prove Property 10 that we claimed at the beginning of the construction.

Proof of Property 10: Consider an arbitrary pair with partition point α and the set Φ of its child-pairs. Consider an internal-pair $\phi \in \Phi$. Note that the length of a child-pair is determined by its corresponding partition piece. According to the construction, except for the near-empty piece incident on α , the length of any non-empty piece is at most twice and at least half the length of another one. Thus, except for the sibling pairs generated by the piece incident on α , the length of any pair $\varphi \prec \phi$ is at least half of the length of ϕ . Finally, the piece incident on α only induces two leaf-pairs and has the maximum length among other empty pieces of ϕ according to Corollary 13. Hence, we have proven the property. \blacktriangleleft

Finally, we summarize the properties of half-empty, near-empty, and empty pieces below.

Property 14. Consider an internal-pair ϕ with partition point set \mathcal{A}_ϕ . Suppose the length of ϕ is δ . The pieces determined by \mathcal{A}_ϕ have the following properties.

- The sum of lengths of empty pieces is less than $2\delta/d_0$.
- There are two near-empty pieces with sum of lengths less than $3\delta/d_0$.
- There is one half-empty piece with length less than δ/d_0 .
- The sum of lengths of empty, near-empty and half-empty pieces is less than $6\delta/d_0$.

Proof. Consider the first property. Suppose $\beta \in \phi$ and β is an apex point. There are two kinds of empty pieces. One is the short pieces and the other is a piece incident on β (denoted by $\xi\beta$). First, the sum of lengths of the short pieces is less than δ/d_0 . Because the length of each short piece is less than δ/n^2 and there are less than n short pieces where $n > d_0$ is the number of partition points in $\hat{\mathcal{A}}$ after projection and before refinement. On the other hand, we prove that the length of $\xi\beta$ is less than δ/d_0 . If β is the first point in ϕ (refer to $\phi = (\beta, \alpha_1)$ in Figure 10), according to refinement (the first refinement case), the length of $\xi\beta$ is less than δ/d_0 . Next consider the case that β is the second point in ϕ $\phi = (\alpha_1, \beta)$ in Figure 10). Suppose ϕ shares the point β with its sibling φ . Hence, ϕ and φ share the point β and β is the first point in φ . Denote the piece of φ incident on β by $\eta\beta$. In this case, we have that ϕ and φ have the same length and $|\xi\beta| = |\eta\beta|$. Since β is the first point in φ , we have proven that $|\eta\beta| \leq \delta/d_0$. Thus, $|\xi\beta| \leq \delta/d_0$.

Algorithm 2: Construct the Yao-Yao graph

Data: A point set \mathcal{P} and an integer $k \geq 2$

Result: $\mathbb{Y}\mathbb{Y}_{2k+1}(\mathcal{P})$

```
1 Initialize:  $\theta = 2\pi/(2k+1)$  and two empty graphs  $\mathbb{Y}_{2k+1}$  and  $\mathbb{Y}\mathbb{Y}_{2k+1}$  ;
2 foreach point  $u$  in  $\mathcal{P}$  do
3   foreach  $j$  in  $[0, 2k]$  do
4     Select  $v$  in  $C_u(j\theta, (j+1)\theta]$  such that  $|uv|$  is the shortest ;
5     Add edge  $\vec{uv}$  into  $\mathbb{Y}_{2k+1}$  ;
6 foreach point  $u$  in  $\mathcal{P}$  do
7   foreach  $j$  in  $[0, 2k]$  do
8     Select  $v$  in  $C_u(j\theta, (j+1)\theta]$ ,  $\vec{vu} \in \mathbb{Y}_{2k+1}$  such that  $|uv|$  is the shortest ;
9     Add edge  $\vec{vu}$  into  $\mathbb{Y}\mathbb{Y}_{2k+1}$  ;
10 return  $\mathbb{Y}\mathbb{Y}_{2k+1}$  ;
```

Consider the second property. Suppose α is a partition point and β is an apex point, and $\alpha, \beta \in \phi$. First, consider the near-empty piece incident on α . If ϕ is the first internal-pair of its parent, according to projection, we add a point λ on the segment of ϕ such that $|\lambda\alpha| = \delta/d_0$. Otherwise, according to Property 10 and 12, we know the piece incident on α is at most $2\delta/d_0$. Second, we consider the other near-empty piece closer to β . Its length is no more than δ/d_0 based on refinement. Thus, the sum of lengths of near-empty pieces is less than $3\delta/d_0$.

For the third property, through refinement, the length of half-empty piece is less than δ/d_0 . Above all, we get the fourth property. \square

4 Hinge Set Decomposition of the Normal Points

All points introduced so far are referred to as normal points and their positions have been defined exactly. Recall that we denote the set of normal points by \mathcal{P}_m^n . In this section, decompose \mathcal{P}_m^n into a collection of sets of points such that each normal point exactly belongs to one set. We call these sets *hinge sets*. See Figure 13 for an overview of the hinge set decomposition.

Based on the hinge sets, the edges among normal points in $\mathbb{Y}\mathbb{Y}_{2k+1}(\mathcal{P}_m^n)$ can be organized in the clear way. For convenience, we regard the Yao-Yao graph as a directed graph. Recall the construction of the directed Yao-Yao graph in Algorithm 2. Note that $C_u(\gamma_1, \gamma_2]$ represents the cone with apex u and consisting of the rays with polar angles in the half-open interval $(\gamma_1, \gamma_2]$ in counterclockwise. We call the first iteration (line 2 to 5) the *Yao-step* and call the second iteration (line 6 to 9) the *Reverse-Yao step*.

Then, we define a *total order* among hinge sets. We call an edge in the Yao-Yao graph a *hinge connection* which connects any two points in the same hinge set or in two adjacent hinge sets w.r.t. the total order. Call other edges *long range connections*. In Section 5, we prove that we can break all long range connections without introducing new ones by adding some auxiliary points. In Section 6, we show that, in the graph with only hinge connections, the shortest path between the two points of the root pair approaches infinity.

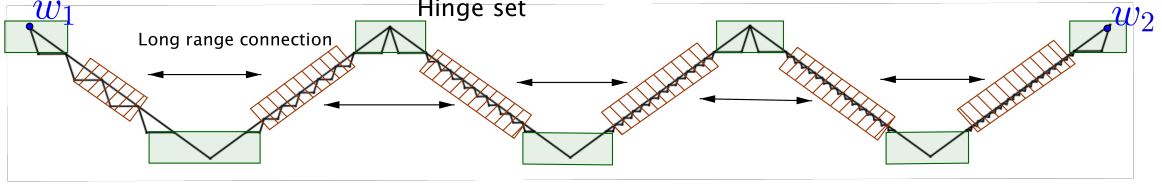


Figure 13: The overview of hinge set decomposition. Roughly speaking, each set of points covered by a green rectangle \square is a hinge set. Recursively, we can further decompose the points covered by shadowed rectangle \square into hinge sets. The hinge connections are the edges between any two points in a hinge set or between two adjacent hinge sets. The other edges in the Yao-Yao graph are long range connections.

4.1 Hinge Set Decomposition

We discuss the process to decompose the set \mathcal{P}_m^n into *hinge sets* such that each point in \mathcal{P}_m^n belongs to exactly one hinge set. Briefly speaking, each hinge set is a set of points which are close geometrically.

Consider a pair $\hat{\phi}$ at *level-l* ($l < m - 1$) with partition point set $\mathcal{A}_{\hat{\phi}}$ and apex point set $\mathcal{B}_{\hat{\phi}}$. Denote the set of the child-pairs of $\hat{\phi}$ by $\hat{\Phi}$. Recall that we say a point u belongs to ϕ (i.e., $u \in \phi$), if the ϕ is (u, \cdot) or (\cdot, u) . Just for convenient to describe, we call some point *center* of a hinge set and other points *affiliated point*. Formally, the hinge sets are defined as follows.

- The hinge set centered on a point $\beta \in \mathcal{B}_{\hat{\phi}}$ such that β belongs to one or two internal-pairs in $\hat{\Phi}$.¹² We denote the two internal-pairs by φ and ϕ .¹³ See Figure 14a for an illustration. The hinge set centered at β includes: β itself, the child-pair of φ closest to β (denote the pair by (ξ_1, ξ_2)) and the child-pair of ϕ closest to β (denoted the pair by (η_1, η_2)). $\xi_1, \xi_2, \eta_1, \eta_2$ are affiliated points. According to the way to determine the leaf-pairs (see Section 3), they only belong to leaf-pairs.
- The hinge set centered on a point $\alpha \in \mathcal{A}_{\hat{\phi}}$ such that α belongs to one or two internal-pairs in $\hat{\Phi}$, or α is an isolated partition point:
 - First, suppose α belongs to one or two internal-pairs in $\hat{\Phi}$, which we denote as φ and ϕ .¹⁴ See Figure 14b. The hinge set centered on α includes: α itself, the two child-pairs closest to α of φ and ϕ (denote the pairs by (ξ_2, ξ_1) and (η_1, η_2)) respectively. $\xi_1, \xi_2, \eta_1, \eta_2$ are affiliated points which only belong to leaf-pairs.
 - Second, α is an isolated point in $\mathcal{A}_{\mathcal{T}}$, i.e., α is an end point of a short piece and does not belong to any internal-pair in $\hat{\Phi}$. See Figure 14c. Then, for each direction of segment of $\hat{\phi}$, we find the closest non-isolated point in $\mathcal{A}_{\hat{\phi}}$. Denote them by α_l and α_r . Merge the two hinge sets centered on α_l and α_r as a new one and add α to the new hinge set.

¹² β must belong to two child-pairs of $\hat{\phi}$ since each β induces two pairs. However, β may belong to two leaf-pairs (i.e., do not belong to any internal-pair). In this case, β is affiliated to a hinge set centered on other point.

¹³ If one of the two child-pairs is a leaf-pair, let $\varphi = \emptyset$.

¹⁴ If α belongs to only one internal-pair of $\hat{\Phi}$, let $\varphi = \emptyset$.

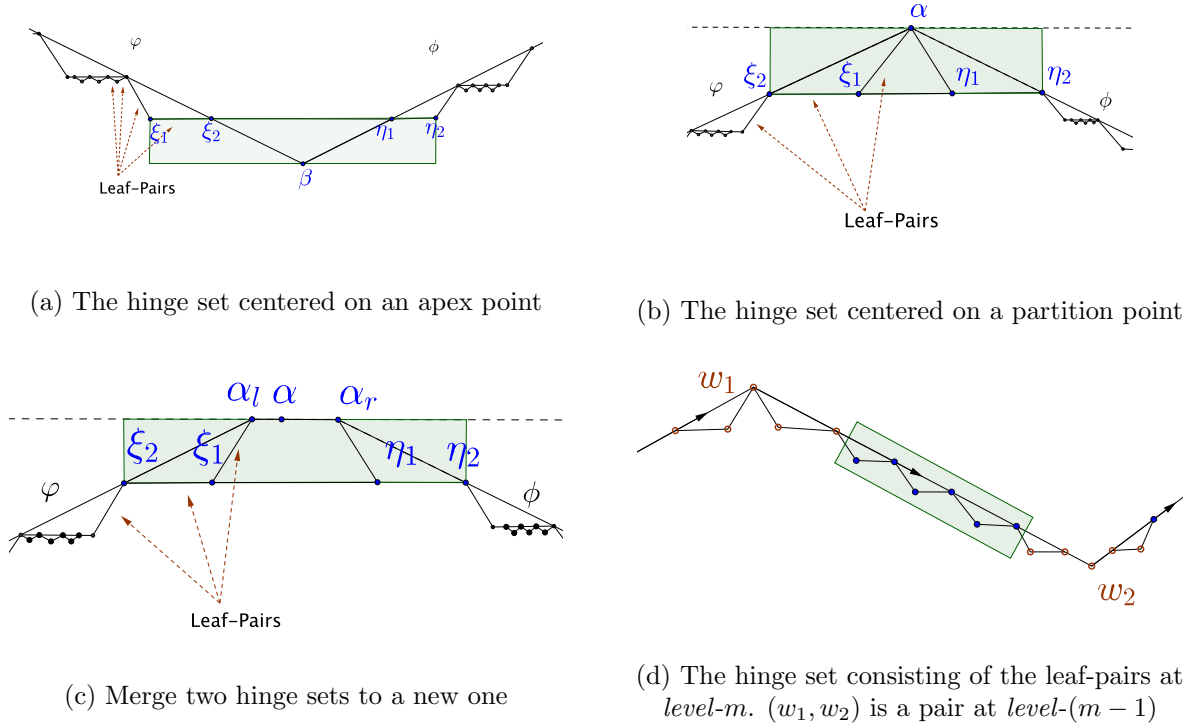


Figure 14: The hinge sets centered on a point in an internal-pair.

W.l.o.g., we process the points μ_1 and μ_2 in the root pair in the same way as the partition points in $\mathcal{A}_{(\mu_1, \mu_2)}$. So far, some points at $level-m$ still do not belong to any hinge set.

- The hinge set consisting of the leaf-pairs at $level-m$: Consider any pair $\phi = (w_1, w_2)$ at $level-(m-1)$. Define the set difference of $\mathcal{A}_\phi \cup \mathcal{B}_\phi$ and the hinge sets centered on w_1 and w_2 as a hinge set.¹⁵ See Figure 14d.

Overall, we decompose the points \mathcal{P}_m^n into a collection of hinge sets.

Lemma 15. Each point p in \mathcal{P}_m^n belongs to exactly one hinge set.

Proof. First, we prove that any two hinge sets are not overlapping. It means that any point in a hinge set does not belong to any other hinge set. First, consider a point λ which only belongs to a leaf-pairs i.e., an affiliated point in the first two type hinge sets (see $\xi_1, \xi_2, \eta_1, \eta_2$ in Figure 14a 14b 14c) or a point in a third type hinge set. It has unique parent-pair ϕ such that $\lambda \in G_\phi$. Let $\phi = (\alpha, \beta)$. If φ is the closest child-pair to α , λ belongs to the hinge set centered on α . Or if φ is the closest child-pair to β , λ belongs to the hinge set centered on β . Otherwise, λ belongs to a third type hinge set. It is not difficult to check that the three cases do non overlap. Thus, point λ belongs to at most one hinge set. Next, consider a point λ which belongs to some internal-pair or is an isolated partition point. Then, λ can only belong to the first two type hinge sets. λ cannot

¹⁵Although these points form the leaf-pairs at $level-m$, these leaf-pairs are the “candidate internal-pairs” to generate the points at $level-(m+1)$.

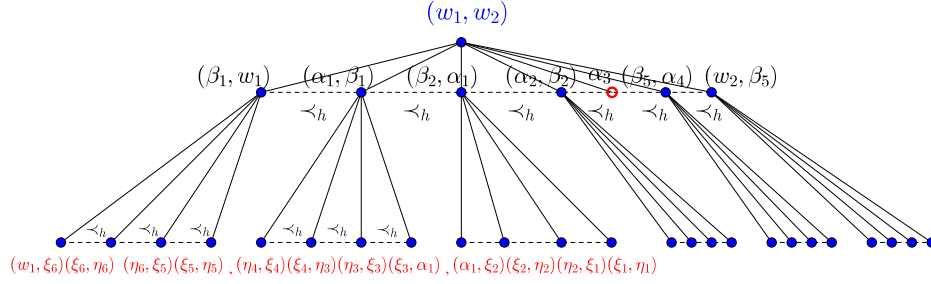


Figure 15: The illustration for order \prec_h . In the example, notice that the order of the *level-2* in \mathcal{T}^R is different with the order in \mathcal{T} (see Figure 5).¹⁶

be a affiliated point for any hinge set since affiliated point only belongs to leaf-pairs. Besides, according to the definition, the hinge set centered on λ is unique. Therefore, λ belongs to at most one hinge set.

On the other hand, we prove that each point in \mathcal{P}_m^n belongs to at least one hinge set. First, any point of *level- m* belongs to a hinge set according to the third case. Second, consider a point λ on *level- l* , $l < m$. If λ belong to any internal-pair, it should be a center of a hinge set. If λ is an isolated partition point, it merges two hinge sets and belongs to the new hinge set. If λ only belongs to a leaf-pair φ and φ is a child-pair of $\phi = (\alpha, \beta)$, then, based on the way to determine the leaf-pairs, λ belongs to hinge set centered on α or β .

Overall, each point in \mathcal{P}_m^n belongs to exactly one hinge set. \square

Order of the hinge sets: We define the total order of all hinge sets. We denote the order by “ \prec_h ”, which is different from the previous order “ \prec ”. The \prec_h is in fact consistent with the order of traversing the fractal path from μ_1 to μ_2 . Rigorously, we define \prec_h below. For comparison, in Figure 15, we reorganize the tree in Figure 5 according to the order \prec_h .

First, consider the root pair (μ_1, μ_2) . We denote the hinge set centered on μ_1 by Λ_{μ_1} and denote the hinge set centered on μ_2 by Λ_{μ_2} . Define Λ_{μ_1} as the first hinge set and Λ_{μ_2} as the last hinge set w.r.t. \prec_h . Then, $\Lambda_{\mu_1} \prec_h \Lambda_{\mu_2}$.

Second, we define the orders of other hinge sets. Consider an internal-pair ϕ with parent pair (w_1, w_2) (or (w_2, w_1)) and $\Lambda_{w_1} \prec_h \Lambda_{w_2}$. Note that there are two hinge sets centered on the points in ϕ respectively. We call the one closer to (in Euclidean distance) Λ_{w_1} the *former hinge set* of ϕ , denoted by $\Lambda_{\phi}^{(-)}$. Call the other the *latter hinge set* of ϕ , denoted by $\Lambda_{\phi}^{(+)}$. Let $\Lambda_{w_1} \prec_h \Lambda_{\phi}^{(-)} \prec_h \Lambda_{\phi}^{(+)} \prec_h \Lambda_{w_2}$. Besides, recall that for any internal-pair ϕ at *level- $(m-1)$* , the points in $\mathcal{A}_{\phi} \cup \mathcal{B}_{\phi}$ but not in $\Lambda_{\phi}^{(-)} \cup \Lambda_{\phi}^{(+)}$ also form a hinge set. We denote it by Λ_{ϕ} and define $\Lambda_{\phi}^{(-)} \prec_h \Lambda_{\phi} \prec_h \Lambda_{\phi}^{(+)}$.

Note that we have organized all pairs in the recursion tree \mathcal{T} . We can transform the tree consisting of all **internal nodes** of \mathcal{T} to a topological equivalent tree \mathcal{T}^R which has a different ordering of the nodes. The order of the sibling pairs in \mathcal{T}^R is determined by their Euclidean distances to the former hinge set of their parent. Overall, the ordering \prec_h of the hinge sets can

¹⁶Note that \mathcal{T}^R only contains the internal nodes of \mathcal{T} . Consider that *level-2* nodes still have their child nodes. Thus, we do not remove the pairs on *level-2* in the example.

Algorithm 3: TravelHinge(ϕ): Travel the hinge sets in the tree \mathcal{T}_ϕ^R

```

1 Visit( $\Lambda_\phi^{(-)}$ ) ;
2 if  $\phi$  is at level- $l$  ( $l < m - 1$ ) then
3   |   foreach child-pair  $\varphi$  of  $\phi$  in  $\mathcal{T}_\phi^R$  do
4   |   |   TravelHinge( $\varphi$ ) ;
5 else
6   |   Visit( $\Lambda_\phi$ )
7 Visit( $\Lambda_\phi^{(+)}$ ) ;

```

be defined by a DFS traversing of \mathcal{T}^R . When we reach a pair ϕ at level- l ($l < m - 1$) for the first time¹⁷, we visit its former hinge set $\Lambda_\phi^{(-)}$. Next, we recursively traverse its child-pairs in the order we just defined. Then we return to the pair and visit its latter hinge set $\Lambda_\phi^{(+)}$. When we reach a pair ϕ at level- $(m - 1)$, we visit $\Lambda_\phi^{(-)}$, Λ_ϕ , $\Lambda_\phi^{(+)}$ in order and return.¹⁸ We denote the procedure by TravelHinge(ϕ) and the pseudocode can be found in Algorithm 3.

4.2 Long Range Connection

We call the edges connecting two non-adjacent hinge sets *long range connections*.

Definition 16 (Long range connection). A *long range connection* is an edge connecting two points in two non-adjacent hinge sets.

If there is no long range connection, the total order of the hinge sets corresponds to the ordering of the shortest path from μ_1 to μ_2 in the final construction. It means that each hinge set has at least one point on the shortest path between μ_1 and μ_2 and the order of these points is consistent with \prec_h . However, there indeed exist long range connections among normal points. In order to achieve the above purpose, we should break the edges connecting two non-adjacent hinge sets. Fortunately, the long range connections in \mathcal{P}_m^n have relatively simple form. We claim that after introducing some auxiliary points (in Section 5), we can cut the long range connections without introducing any new long range connections. Hence, only adjacent hinge sets in the above order \prec_h have edges in the Yao-Yao graph.

Now, we examine the long range connections in $\mathbf{YY}_{2k+1}(\mathcal{P}_m^n)$. First, we show that we only need to consider the long range connections between the points in \mathcal{T}_ϕ and \mathcal{T}_φ for any two sibling pairs ϕ and φ . Recall that \mathcal{T}_ϕ denotes the subtree rooted at ϕ (including ϕ). If there exist two points $p \in \mathcal{T}_\phi - \mathcal{T}_\phi \cap \mathcal{T}_\varphi$ and $q \in \mathcal{T}_\varphi - \mathcal{T}_\phi \cap \mathcal{T}_\varphi$ such that pq is a long range connection, we say there is a long range connection between \mathcal{T}_ϕ and \mathcal{T}_φ .

Claim 17. Suppose that for any two sibling pairs ϕ and φ in \mathcal{T} at level- l for $l \leq m - 1$, there is no long range connection between the points in \mathcal{T}_ϕ and \mathcal{T}_φ . Then, there is no long range connection.

¹⁷ level- $(m - 1)$ is the second to last level of \mathcal{T} and the last level of \mathcal{T}^R .

¹⁸ Note that two adjacent sibling pairs share the same hinge set. So the same hinge set may be visited twice, and the two visits are adjacent in the total order. So it does not affect the order between two distinct hinge sets.

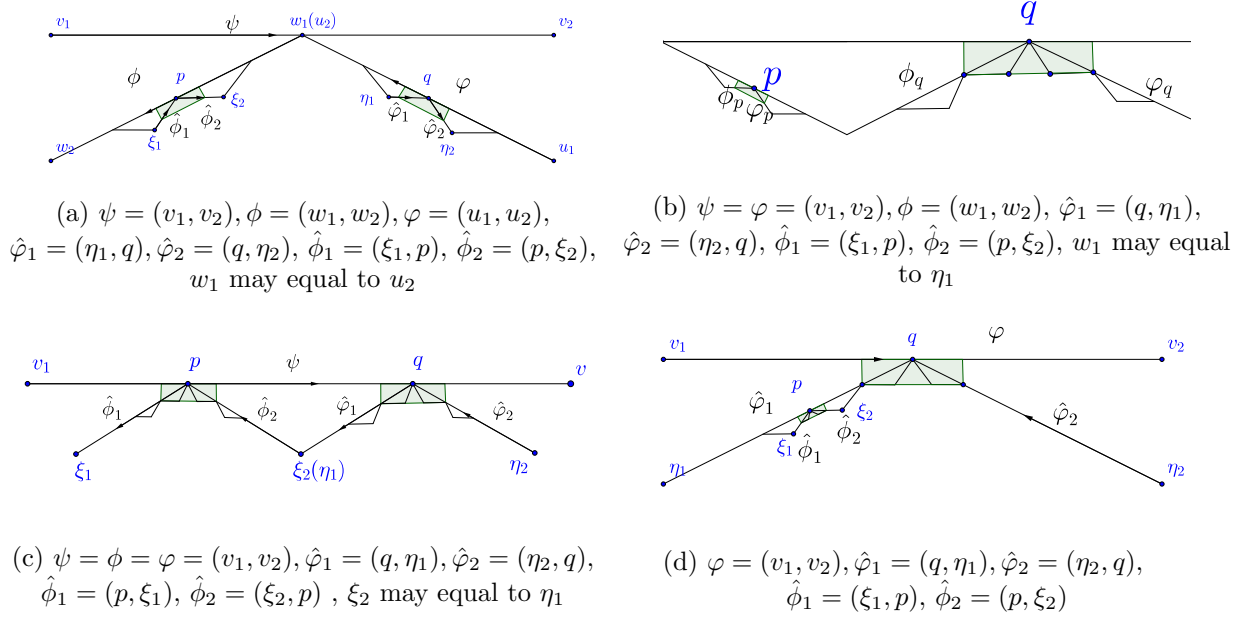


Figure 16: The possible relative positions of p and q . Although, in the figure, p and q are partition points, it does not induce any new case when p or q is an apex point according to our divided condition in the proof.

Proof. Consider two non-adjacent hinge sets Λ_p and Λ_q (if two hinge sets are adjacent, the edges between them are hinge connections) and $\lambda_1 \in \Lambda_p$ and $\lambda_2 \in \Lambda_q$. We prove that we can find two sibling pairs ϕ and φ such that \mathcal{T}_ϕ and \mathcal{T}_φ contains λ_1 and λ_2 respectively. Then, we consider the possible cases about the two non-adjacent hinge sets.

First, we consider the case that each of the two hinge sets is centered on a point of some internal-pair. Denote the two center points by p and q and the two hinge sets by Λ_p and Λ_q . p belongs to one or two adjacent internal-pairs. W.l.o.g., suppose they are $\hat{\phi}_1$ and $\hat{\phi}_2$ ($\hat{\phi}_2 = \emptyset$ if p only belongs to one internal-pair). Meanwhile, q belongs to one or two adjacent internal-pairs. Suppose they are $\hat{\varphi}_1$ and $\hat{\varphi}_2$. W.l.o.g., suppose the level of $\hat{\varphi}_1$ and $\hat{\varphi}_2$ is no more than the level of $\hat{\phi}_1$ and $\hat{\phi}_2$. Then, we distinguish two cases. In the first one, none of $\hat{\varphi}_1$ and $\hat{\varphi}_2$ is an ancestor of $\hat{\phi}_1$ and $\hat{\phi}_2$. Otherwise, it is the second case.

Consider the first case. Suppose the closest common ancestor of $\hat{\varphi}_1, \hat{\varphi}_2, \hat{\phi}_1$ and $\hat{\phi}_2$ is pair ψ in \mathcal{T} . If p and q do not belong to $\mathcal{A}_\psi \cup \mathcal{B}_\psi$, there are two different child-pairs ϕ and φ of ψ (see Figure 16a), such that Λ_p belongs to \mathcal{T}_ϕ and Λ_q belongs to \mathcal{T}_φ . Since points between \mathcal{T}_ϕ and \mathcal{T}_φ have no long range connection according to the assumption, points between Λ_p and Λ_q have no long range connection. Then consider the case that q belongs to $\mathcal{A}_\psi \cup \mathcal{B}_\psi$ (see Figure 16b). Note that Λ_q is a subset of $\mathcal{T}_{\hat{\varphi}_1} \cup \mathcal{T}_{\hat{\varphi}_2}$. Because there is no long range connections for the points between $\mathcal{T}_{\hat{\varphi}_1}, \mathcal{T}_{\hat{\varphi}_2}$ and \mathcal{T}_ϕ , Λ_p and Λ_q have no long range connection. Finally, if both p and q belong to $\mathcal{A}_\psi \cup \mathcal{B}_\psi$ (see Figure 16c), since there is no long range connection for points between $\mathcal{T}_{\hat{\phi}_1}, \mathcal{T}_{\hat{\phi}_2}$ and $\mathcal{T}_{\hat{\varphi}_1}, \mathcal{T}_{\hat{\varphi}_2}$, Λ_p and Λ_q have no long range connection.

Consider the second case. See Figure 16d. W.l.o.g., suppose $\hat{\phi}_1$ and $\hat{\phi}_2$ are in the subtree of $\mathcal{T}_{\hat{\varphi}_1}$. Λ_q is a subset of $\mathcal{T}_{\hat{\varphi}_1} \cup \mathcal{T}_{\hat{\varphi}_2}$. Moreover, according to the assumption, the points between $\mathcal{T}_{\hat{\varphi}_1}$

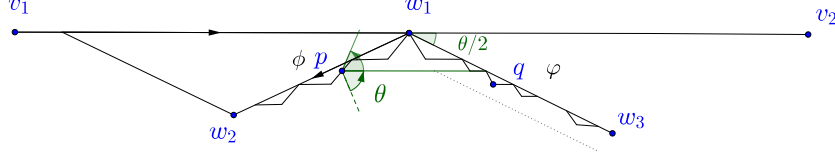


Figure 17: The points of \mathcal{T}_φ locate in at most two cones of p .

and $\mathcal{T}_{\hat{\varphi}_2}$ have no long range connections. Since $\hat{\phi}_1$ and $\hat{\phi}_2$ are in the subtree of $\mathcal{T}_{\hat{\varphi}_1}$, we know that the points in $\Lambda_q \cap \mathcal{T}_{\hat{\varphi}_2}$ have no long range connections to Λ_p . Then we consider the long range connection between $\Lambda_q \cap \mathcal{T}_{\hat{\varphi}_1}$ and Λ_p . Actually, it is reduced to the first case, thus they have no long range connection.

Above all, we have discussed the case that each of the two hinge sets is centered on a point of some internal-pair. Next, suppose that at least one of the hinge sets is a third type hinge set which contains only leaf-pairs at *level-m*. If both of them are the third type hinge sets, denoted by Λ_ϕ and Λ_φ , there must exist two sibling pairs $\hat{\phi}$ and $\hat{\varphi}$ such that $\Lambda_\phi \in \mathcal{T}_{\hat{\phi}}$ and $\Lambda_\varphi \in \mathcal{T}_{\hat{\varphi}}$. According to the hypothesis that there is no long range connection between the points in $\mathcal{T}_{\hat{\phi}}$ and $\mathcal{T}_{\hat{\varphi}}$, there is no long range connection between Λ_ϕ and Λ_φ . Finally, consider the case that there is only one third type hinge set, denoted by Λ_ϕ and the other is centered on q , denoted by Λ_q . Suppose q is the shared point of $\hat{\varphi}_2$ and $\hat{\varphi}_1$. We distinguish two cases according to whether $\phi \in \mathcal{T}_{\hat{\varphi}_1} \cup \mathcal{T}_{\hat{\varphi}_2}$ or not. As we have discussed above, we can prove that there is no long range connection between Λ_q and Λ_ϕ . \square

According to Claim 17, next, we discuss the possible long range connections between \mathcal{T}_ϕ and \mathcal{T}_φ for two sibling pairs ϕ and φ . Suppose p belongs to \mathcal{T}_ϕ and q belongs to \mathcal{T}_φ . In the following, we prove that if the directed edge \overrightarrow{pq} is an edge in $\mathbb{Y}\mathbb{Y}_{2k+1}(\mathcal{P}_m^n)$, then $\phi \prec \varphi$. Moreover, note that the points of \mathcal{T}_φ locate in at most two cones of p . See Figure 17 for an illustration. $p \in \mathcal{T}_\phi$ and \mathcal{T}_φ locates in two cones of p according to the angular relation. We prove that for each point p , only one of the two cones may contain a long range connection. Intuitively, these properties (Observation 18, Lemma 19 and 20) result from Property 6 which does not hold for even Yao-Yao graphs.

We prove the properties formally below. Consider two sibling pairs $\phi \prec \varphi$. First, suppose φ is a leaf-pairs (see Observation 18). Second, we consider that φ is an internal-pair (see Lemma 19 and 20).

Observation 18. Consider two sibling pairs ϕ and φ such that $\phi \prec \varphi$. If φ is a leaf-pair, there is no long range connection between \mathcal{T}_ϕ and \mathcal{T}_φ (i.e., φ itself).

Proof. See Figure 18 for an illustration. Suppose $\varphi = (w_3, w_1)$. First, we consider the case that ϕ and φ share one point. Let $\phi = (w_1, w_2)$. Then, $\mathcal{T}_\phi \cap \mathcal{T}_\varphi = w_1$. We should prove that for any $p \in \mathcal{T}_\phi - w_1$ (i.e., $p = p^{(1)}$ in Figure 18), there is no edge pw_3 in Yao-Yao graph. Let (η_1, η_2) be the pair in \mathcal{G}_ϕ closest to w_1 . There is no edge $\overrightarrow{w_3p}$ in the Yao-step since η_2 and p are in the same cone of w_3 and $|\eta_2 w_3| < |p w_3|$. Note that $\eta_2 w_3$ is a hinge connection. If directed edge $\overrightarrow{pw_3}$ is accepted in the Yao-step, $\overrightarrow{pw_3}$ cannot be accepted in the reverse-Yao step since $\overrightarrow{\eta_2 w_3}$ exists in the Yao-step, and

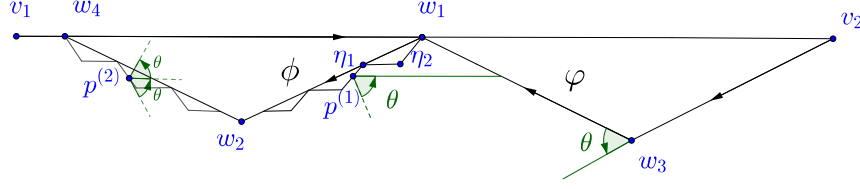


Figure 18: ϕ and φ are sibling pairs such that $\phi \prec \varphi$. φ is a leaf-pair. There is no long range connection between \mathcal{T}_ϕ and the points of \mathcal{T}_φ (i.e., φ itself).

η_2 and p are in the same cone of w_3 and $|\eta_2 w_3| < |p w_3|$. Thus, there is no long range connection between \mathcal{T}_ϕ and φ .

Second, we consider the case that ϕ and φ do not overlap, i.e., $\mathcal{T}_\phi \cap \mathcal{T}_\varphi = \emptyset$. W.l.o.g., let $\phi = (w_2, w_4)$ and $p \in \phi$ (i.e., $p = p^{(2)}$). Similar to the first case, we can prove that there is no long range connection $p w_3$. Then we consider the point w_1 . There is edge from w_1 to p in the Yao-step since η_1 and p are in the same cone of w_1 and $|w_1 \eta_1| < |w_1 p|$. Besides, if directed edge $\overrightarrow{p w_1}$ is accepted in the Yao-step, $\overrightarrow{p w_1}$ cannot be accepted in the reverse-Yao step since $\overrightarrow{\eta_1 w_1}$ exists in the Yao-step and $|\eta_1 w_1| < |p w_1|$. \square

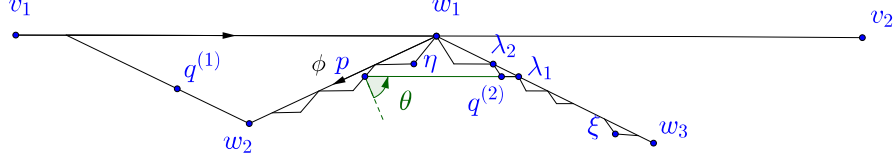
Given a pair (v_1, v_2) with child-pair set Φ , consider two sibling pairs ϕ and φ in Φ where $\phi = (w_1, w_2)$. For convenience, let $\angle u_1 u_2$ be the polar angle of vector $u_1 u_2$. Let $\angle(u_1 u_2, v_1 v_2)$ be $\angle v_1 v_2 - \angle u_1 u_2$, i.e., the angle from $u_1 u_2$ to $v_1 v_2$ in the counterclockwise direction.

Recall that there are two kinds of normal points according to the definition of gadget: partition points and apex points. According to the type of point w_1 and the relative position between $\phi = (w_1, w_2)$ and (v_1, v_2) , there are four cases: (1) w_1 is a partition point and ϕ is on the right side of $v_1 v_2$, (2) w_1 is an apex point and ϕ is on the left side of $v_1 v_2$, (3) w_1 is a partition point and ϕ is on the left side of $v_1 v_2$, (4) w_1 is an apex point and ϕ is on the right side of $v_1 v_2$. See Figure 19 and 21 for illustrations.

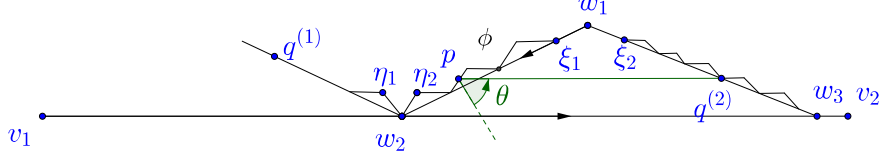
We prove the possible long range connections between the points of \mathcal{T}_ϕ and \mathcal{T}_φ case by case. Lemma 19 covers case (1) and case (2) which satisfy the condition $\angle(v_1 v_2, w_2 w_1) = \theta/2$. Lemma 20 covers case (3) and case (4) which satisfy the condition $\angle(v_1 v_2, w_2 w_1) = -\theta/2$.

Lemma 19. Given a pair (v_1, v_2) with child-pair set Φ , consider two sibling pairs ϕ and φ in Φ where $\phi = (w_1, w_2)$. ϕ and φ are at *level-l* for $l \leq m - 1$. Suppose point p belongs to \mathcal{T}_ϕ and q belongs to \mathcal{T}_φ . If $\angle(v_1 v_2, w_2 w_1) = \theta/2$ and there is a directed edge from p to q in $\mathbb{Y}\mathbb{Y}_{2k+1}(\mathcal{P}_m^n)$, then $\angle(v_1 v_2, pq) = 0$ (i.e., pq is parallel to $v_1 v_2$), and q is a point in the gadget \mathbf{G}_φ generated by φ .

Proof. As we have discussed above, there are two cases under the conditions. Consider case (1). See Figure 19a. First, we prove that $\angle(v_1 v_2, pq)$ should belong to $(-\theta/2, 0]$. If q belongs to \mathcal{T}_φ and $\varphi \prec \phi$ (i.e., $q = q^{(1)}$ in Figure 19a), w_2 and q are in the same cone of p . There is no edge from p to q since $|p w_2| < |p q|$ and the edge $p q$ is rejected in the Yao-step. Then consider that q belongs to \mathcal{T}_φ and $\varphi \succ \phi$ (i.e., $q = q^{(2)}$ in Figure 19a). According to Observation 18, we safely assume that φ is an internal-pair. Denote the point in \mathbf{G}_ϕ closest to w_1 by η . If $\angle(v_1 v_2, pq) > 0$, η and q are in the same cone of p since $w_1 \eta$ has the maximum length among its sibling pairs according to Corollary 13. Thus, there is no edge from p to q in the Yao-step since $|p \eta| < |p q|$. Thus, $\angle(v_1 v_2, pq) \in (-\theta/2, 0]$. Then, we prove that $\angle(v_1 v_2, pq) = 0$. Suppose the projection point of p to pair φ is λ_1 (the λ_1

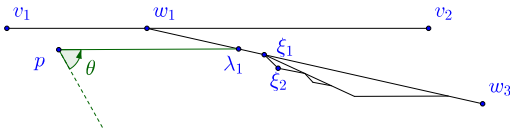


(a) Case 1: w_1 is the partition point and ϕ is on the right side of v_1v_2

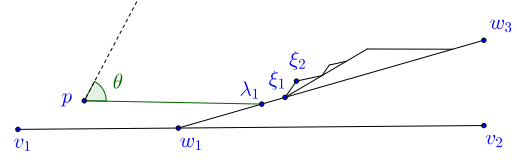


(b) Case 2: w_1 is the apex point and ϕ is on the left side of v_1v_2

Figure 19: The two cases about $\angle(v_1v_2, w_2w_1) = \theta/2$. Here $\phi = (w_1, w_2)$ and $p \in \mathcal{T}_\phi$.



(a) The degenerated case of case 1 in Lemma 19



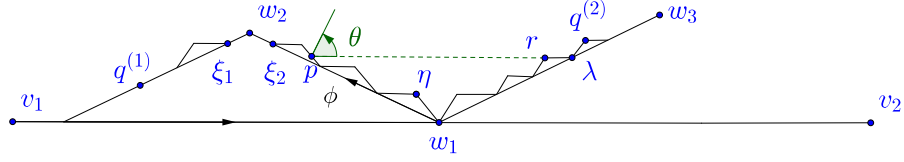
(b) The degenerated case of case 3 in Lemma 20

Figure 20: The degenerated cases in which the projection point of p is an isolated partition point, i.e., λ_1 in the figure is an isolated partition point which is incident on a short piece.

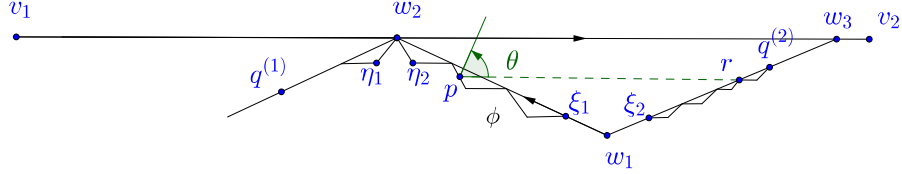
must exist according to the projection process) and $q^{(2)}$ is an apex point of the piece $\lambda_1\lambda_2$. Note that $\theta < \pi/3$ for $k \geq 3$ and the maximum length among child internal-pairs of φ is at most twice longer than the minimum one (see Property 10). It is not difficult to check that the point closest to p in cone $C_p(-\theta, 0]$ is $q^{(2)}$. Thus, $q = q^{(2)}$ and pq is parallel to v_1v_2 .

Note that there is a degenerated case in which the projection λ_1 is an end point of an empty piece. Thus, we do not generate the corresponding apex point q . See Figure 20a for an illustration. (ξ_2, ξ_1) is the pair closest to λ_1 . Note that for $k \geq 3$, the angle $\angle p\lambda_1\xi_2 > \pi/2$ and (ξ_1, ξ_2) is a leaf. Thus, in this degenerated case, the point closest to p in cone $C_p(-\theta, 0]$ is λ_1 . $p\lambda_1$ is also parallel to v_1v_2 . Thus, the lemma is still true. We can process the degenerated case in the same framework in the following and do not distinguish the degenerated case particularly.

Consider case (2). See Figure 19b. Suppose η_2 is the apex point of the near-empty piece of ϕ incident on w_2 . Note that $w_2\eta_2$ has the maximum length among its sibling pairs. If q belongs to \mathcal{T}_φ and $\varphi \prec \phi$ (i.e., $q = q^{(1)}$ in Figure 19b), η_2 and q are in the same cone of p and $|\eta_2p| < |qp|$. Thus, there is no edge from p to q in the Yao-step. Then consider that q belongs to \mathcal{T}_φ and $\varphi \succ \phi$ (i.e., $q = q^{(2)}$ in Figure 19b). According to Observation 18, we assume that φ is an internal-pair. If $\varphi \succ \phi$, the polar angle of pq should belong to $(-\theta/2, 0]$. If not, w_1 and q are in the same cone. Thus, there is no edge from p to q in the Yao-step since $|pq| > |pw_1|$. Then we prove that pq is



(a) Case 3: w_1 is the partition point and ϕ is on the left side of v_1v_2



(b) Case 4: w_1 is the apex point and ϕ is on the right side of v_1v_2

Figure 21: The two cases about $\angle(v_1v_2, w_2w_1) = -\theta/2$. Here $\phi = (w_1, w_2)$ and $p \in \mathcal{T}_\phi$.

parallel to v_1v_2 . The point closest to p in the cone $C_p(-\theta, 0]$ is the projection point of p (p must exist because of the projection). Thus, pq is parallel to v_1v_2 . \square

Lemma 20. Given a pair (v_1, v_2) with child-pair set Φ , consider two sibling pairs ϕ and φ in Φ where $\phi = (w_1, w_2)$. Suppose ϕ and φ are at level- l for $l \leq m-1$. Suppose point p belongs to \mathcal{T}_ϕ , and q belongs to \mathcal{T}_φ . If $\angle(v_1v_2, w_2w_1) = -\theta/2$ and there is a directed edge from p to q in $\mathcal{YY}_{2k+1}(\mathcal{P}_m^n)$, then $\angle(v_1v_2, pq) \in (0, \theta/2)$. Moreover, there exists a point r in \mathcal{T}_φ such that pr is parallel to v_1v_2 and $|pr| < |pq|$. Moreover, r is a point in the gadget G_φ generated by φ .

Proof. As we have discussed above, case (3) and (4) satisfy the condition $\angle(v_1v_2, w_2w_1) = -\theta/2$. Suppose q belongs to \mathcal{T}_φ . Consider case (3). See Figure 21a. Suppose $w_2\xi_1$ and $w_2\xi_2$ are the two empty pieces incident on w_2 . If q is in \mathcal{T}_φ and $\varphi \prec \phi$ (i.e., $q = q^{(1)}$ in Figure 21a), ξ_1 and q are in the same cone of p . If q is not ξ_1 , there is no edge from p to q even in the Yao-step since $|p\xi_1| < |pq|$. If q is ξ_1 , $p\xi_1$ would not be accepted by ξ_1 in the reverse-Yao step, since there is an edge from ξ_2 to ξ_1 and $|\xi_1\xi_2| < |p\xi_1|$. Then consider that q (i.e., $q = q^{(2)}$ in Figure 21a) is in \mathcal{T}_φ and $\varphi \succ \phi$. According to Observation 18, we safely assume that φ is an internal-pair. Thus, $\angle(v_1v_2, pq) \in [-\theta/2, \theta/2)$. If $\angle(v_1v_2, pq) \in [-\theta/2, 0]$, pq is not a directed edge in Yao-step since w_1 and q are in the same cone and $|w_1p| < |pq|$. Finally, consider the projection point λ (λ exists because of the projection) of p to pair φ . r is the apex point related to λ and on the segment $p\lambda$. It is not difficult to check that $|pr| < |pq|$ since $\theta/2 \leq \pi/2$ and the maximum length among the non-empty pieces of φ is at most twice longer the minimum one (according to refinement). Similar to case 1 in Lemma 19, these is a degenerated case that λ is the end point of an empty piece. See Figure 20b. In this case, it is not difficult to check $|p\lambda| < |pq|$.

Consider case (4). See Figure 21b. Suppose η_1 and η_2 are the apex points of the near-empty pieces incident on w_2 . If q is in \mathcal{T}_φ and $\varphi \prec \phi$ (i.e., $q = q^{(1)}$ in Figure 21b), η_1 and q are in the same cone of p . If q is not η_1 , there is no edge from p to q in the Yao-step since $|p\eta_1| < |pq|$. If q is η_1 , $p\eta_1$ would not be accepted by η_1 in the reverse-Yao step since there is an edge from η_2 to η_1 and $|\eta_1\eta_2| < |p\eta_1|$. Then consider q is in \mathcal{T}_φ and $\varphi \succ \phi$ (i.e., $q = q^{(2)}$ in Figure 21b). Based on Observation 18, we assume that φ is an internal-pair. The polar angle of pq should

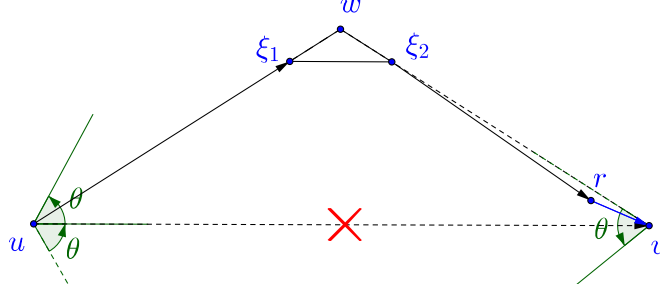


Figure 22: A simple example to explain how an auxiliary point cuts a long range connection.

belong to $(0, \theta/2)$. If not, w_1 and q are in the same cone. Thus, there is no edge from p to q since $|pq| > |pw_1|$. Finally, consider the projection point r of p (r must exist because of the projection) to pair φ . $|pr| < |pq|$ and pr is parallel to v_1v_2 since $\theta/2 \leq \pi/2$. \square

In the next section, we discuss how to cut such long range connections. Roughly speaking, under the condition of Lemma 19, we can cut the long range connection pq through adding two auxiliary points close to q . Under the condition of Lemma 20, we can cut the long range connection pq through adding two auxiliary points close to r .

Based on Lemma 19 and 20, we have the following corollary.

Corollary 21. Consider two sibling pairs ϕ and φ with subtrees \mathcal{T}_ϕ and \mathcal{T}_φ respectively. Suppose p belongs to \mathcal{T}_ϕ and q belongs to \mathcal{T}_φ . If directed edge \vec{pq} is in $\mathbb{Y}\mathbb{Y}_{2k+1}(\mathcal{P}_m^n)$, then $\phi < \varphi$.

5 The Positions of Auxiliary Points

We discuss how to use the auxiliary points to cut the long range connections in the Yao-Yao graph $\mathbb{Y}\mathbb{Y}_{2k+1}(\mathcal{P}_m^n)$. According to Claim 17, it is sufficient by cutting all long range connections between siblings. Denote the set of auxiliary points by \mathcal{P}_m^a . Let $\mathcal{P}_m = \mathcal{P}_m^n \cup \mathcal{P}_m^a$.

First, we consider a simple example to see how auxiliary points work. Consider three points u , v and w . Line uv is horizontal, and $\angle wvu = \angle wuv = \theta/2$. The point ξ_1 and ξ_2 are two points on segment uw and vw respectively. $\xi_1\xi_2$ is horizontal. See Figure 22. Note that the polar angles of a cone in the Yao-Yao graph belong to a half-open interval in the counterclockwise direction. Thus, uv is in the $\mathbb{Y}\mathbb{Y}_{2k+1}$ graph, which is the shortest path between u and v . However, we can add an auxiliary point r close to v and $\angle rvu < \theta/2$. Then according to the definition of Yao-Yao graphs, the point v rejects the edge uv in the reverse-Yao step since rv exists in the Yao-step, and point r and u are in the same cone of v and $|rv| < |vu|$. Then, consider ur and $r\xi_1$. The directed edge ur is not in Yao graph since ξ_1 and r are in the same cone of u and $|\xi_1u| < |ur|$. The directed edge ru is not in Yao graph since ξ_1 and u are in the same cone of r and $|\xi_1r| < |ur|$. Besides, directed edge ξ_1r is not in the Yao graph since r and ξ_2 are in the same cone of ξ_1 and $|\xi_1\xi_2| < |\xi_1r|$. Finally, directed edge $r\xi_1$ is not accepted by ξ_1 in the reverse-Yao step since there is an edge $\xi_2\xi_1$ in the same cone of r and $|\xi_2\xi_1| < |r\xi_1|$. Overall, the shortest path between uv becomes $u\xi_1\xi_2rv$.

The positions of the auxiliary points: Inspired by the example in Figure 22, we call the normal point closest to an auxiliary point the *center* of the auxiliary point. Then, we find *candidate centers* to add auxiliary points.

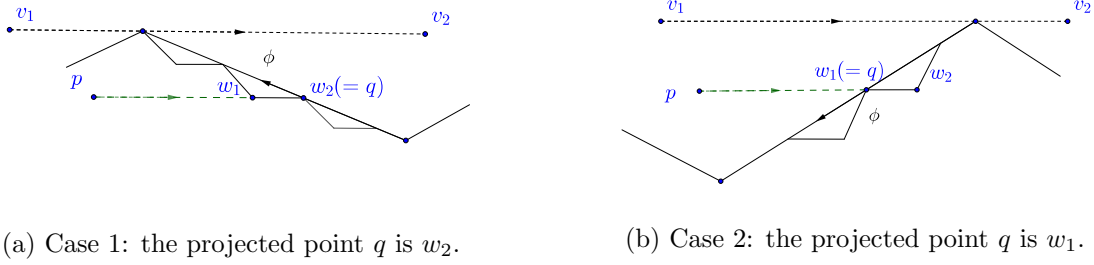


Figure 23: The illustration for candidate center of p .

Lemma 22 (Candidate center). Given a pair (v_1, v_2) with its child-pair set Φ , consider two sibling pairs $\varphi, \phi \in \Phi$ and $\varphi \prec \phi$. Suppose p is a point in \mathcal{T}_φ and its projected point (denoted by q) on the segment of ϕ along direction $\overrightarrow{v_1 v_2}$. Then, there exists a nonempty subset $\mathcal{S} \subseteq \mathcal{G}_\phi$ such that for any $u \in \mathcal{S}$, pu is parallel to $v_1 v_2$. See Figure 23 for an illustration.

We call the point $u := \arg \min_{u \in \mathcal{S}} |pu|$ a *candidate center* of ϕ . Note that the candidate center may not be the projected point q .

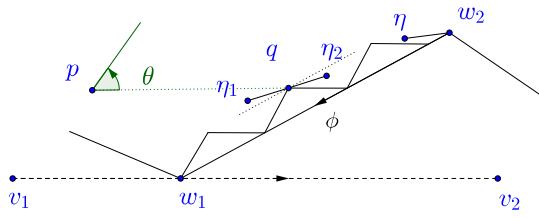
Proof. The correctness directly results from the projection process. In the first case (see Figure 23a) where the apex points of \mathcal{G}_ϕ and p are in the same side of segment of ϕ , we will generate a pair (w_1, w_2) such that $q = w_2$ and pw_1 and pw_2 are parallel to $v_1 v_2$. Thus, $\mathcal{S} = \{w_1, w_2\}$ and we call the point w_1 a candidate center of ϕ . Note that w_1 is not the projected point of p . In the second case (see Figure 23b) where the apex points of \mathcal{G}_ϕ and p are on the different sides of segment of ϕ , we will generate a pair (w_1, w_2) such that $q = w_1$ and pw_1 and pw_2 are parallel to $v_1 v_2$. Thus, $\mathcal{S} = \{w_1, w_2\}$ and we call the point w_1 a candidate center of ϕ . Beside, q may be an isolated partition point or a point in ϕ , then \mathcal{S} and the candidate center is point q itself. \square

Definition 23 (Candidate center set of ϕ). Consider a pair ϕ with parent pair (v_1, v_2) . Let Φ be the set of child-pairs of (v_1, v_2) . In the projection process, we project all points $p \in \bigcup_{\varphi \prec \phi, \varphi \in \Phi} \mathcal{T}_\varphi$ to the segment of ϕ along the direction $v_1 v_2$. Each such point p whose projected point falls inside the segment of ϕ corresponds to a candidate center of ϕ defined in Lemma 22. We call the set consisting of all these candidate centers the *candidate center set* of ϕ . Note that candidate center set is a subset of \mathcal{G}_ϕ .

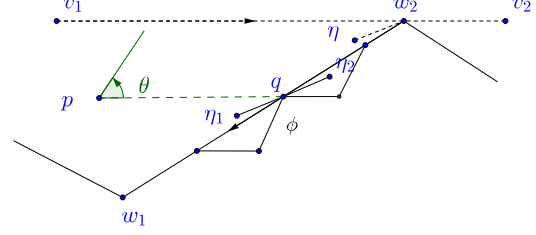
We add some auxiliary points centered on these candidate centers to break long range connection. For convenience, we define some parameters first. Let Δ be the minimum distance between any two normal points and n be the number of the normal points. Recall that we partition the root pair μ_1, μ_2 into d_0 equidistant pieces. Let γ be a very small angle, such as $\gamma = \theta d_0^{-1}$. Let $\sigma = \max\{\sin(\theta/2 - \gamma)/\sin \gamma, \sin^{-1}(\theta/2 - \gamma)\} + \epsilon$ for some small $\epsilon > 0$. Let $\chi = d_0 \sigma^n \Delta^{-1}$. Roughly speaking, $\chi \gg d_0 > \sigma > 1$.

We traverse \mathcal{T} in the DFS preorder. Each time we reach a pair ϕ , we find all candidate centers in \mathcal{G}_ϕ and add auxiliary points centered on them.¹⁹ Moreover, let the order of ϕ in the DFS preorder w.r.t. \mathcal{T} be κ . The distance between the auxiliary point and its center q depends on κ . We use the polar coordinate to describe the relative location of an auxiliary point to its center.

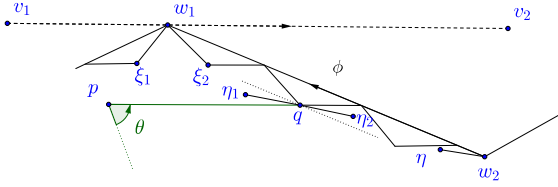
¹⁹Note that the candidate centers belong to \mathcal{G}_ϕ , may not belong to ϕ itself. Besides, here we do not need to distinguish whether the candidate center related to a long range connection or not. It may reduce the number of auxiliary points but do not influent the correctness.



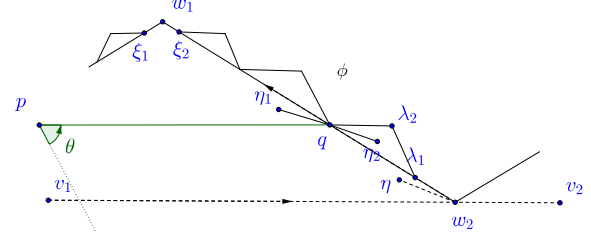
(a) Case 1a: w_1 is the partition point and ϕ is on the left side of v_1v_2



(b) Case 1b: w_1 is the apex point and ϕ is on the right side of v_1v_2



(c) Case 2a: w_1 is the partition point and ϕ is on the right side of v_1v_2



(d) Case 2b: w_1 is the apex point and ϕ is on the left side of v_1v_2

Figure 24: The auxiliary points for each point. Here $\phi = (w_2, w_1)$ and $q \in G_\phi$. η_1 and η_2 are two auxiliary points centered on q . Note that $|\eta_1 q|$ and $|\eta_2 q|$ are very small in fact. This is just a diagram to explain the relative positions between $\{\eta_1, \eta_2\}$ and q .

Let $\phi = (w_2, w_1)$ and (v_1, v_2) be the parent-pair of ϕ . There are two cases according to $\angle(v_1v_2, w_1w_2) = \theta/2$ or $-\theta/2$.

- $\angle(v_1v_2, w_1w_2) = \theta/2$ (see Figure 24a and 24b):
 - If $q = w_1$, do not add auxiliary point.
 - If $q = w_2$, we add the point η such that $\angle(w_2w_1, w_2\eta) = -\gamma$ and $|w_2\eta| = \sigma^\kappa \chi^{-1}$.
 - Otherwise, we add two points η_1 and η_2 centered on q such that $\angle(w_2w_1, q\eta_1) = \angle(w_2w_1, \eta_2q) = -\gamma$ and $|q\eta_1| = |\eta_2q| = \sigma^\kappa \chi^{-1}$.
- $\angle(v_1v_2, w_1w_2) = -\theta/2$ (see Figure 24c and 24d):
 - If $q = w_1$, do not add auxiliary point.
 - If $q = w_2$, we add the point η such that $\angle(w_2w_1, w_2\eta) = \gamma$ and $|w_2\eta| = \sigma^\kappa \chi^{-1}$.
 - If p and q are in the same hinge set (i.e., p, q are the points ξ_1, ξ_2 in Figure 24c or 24d), we add two points η_1 and η_2 centered on q such that $\angle(w_2w_1, q\eta_1) = \angle(w_2w_1, \eta_2q) = \gamma$ and $|q\eta_1| = |\eta_2q| = \sigma^\kappa \chi^{-1} + \epsilon_0$ where ϵ_0 is much less than the distance between any two points in \mathcal{P}_m .²⁰

²⁰ It is slightly different from the first case. We add two auxiliary points with distance slightly larger than $\sigma^\kappa \chi^{-1}$ to its center when p and q are in the same hinge set. The reason is that the cone is half-open half-close in the counterclockwise direction. It will help a lot to unify the proof in the same framework. See the details in the proof of Lemma 25.

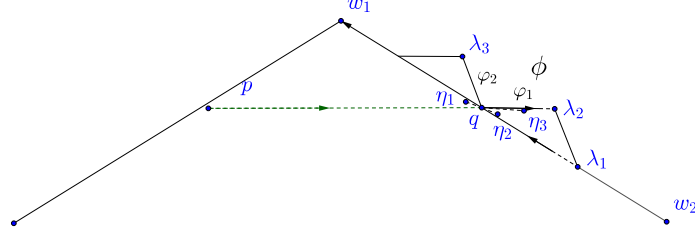


Figure 25: The positions of auxiliary points (η_1, η_2, η_3) centered on normal point q .

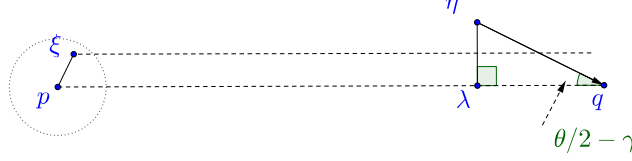


Figure 26: $|\xi p| \leq \sigma^{-1}|\eta q|$ for the auxiliary point of p . Moreover, the perpendicular distance from η to pq (i.e., $|\eta \lambda|$ in the figure) is larger than $|\xi p|$.

- Otherwise, we add two points η_1 and η_2 centered on q such that $\angle(w_2 w_1, q \eta_1) = \angle(w_2 w_1, \eta_2 q) = \gamma$ and $|q \eta_1| = |q \eta_2| = \sigma^\kappa \chi^{-1}$.

First, we list some useful properties of the auxiliary points below.

Property 24. Properties of auxiliary points:

- P1 The maximum length between an auxiliary point and its center is at most $d_0^{-1} \Delta$.
- P2 Any point $q \in \mathcal{P}_m^n$ can become a center for auxiliary points at most twice. Here, for each time that we indeed add some auxiliary points for a candidate center p , we say that p becomes a center once.
- P3 There are at most three auxiliary points centered on a normal point.
- P4 Suppose q is a candidate center because of the projection of p and we add the auxiliary point η centered on q . If there is an auxiliary point ξ centered on p , then $|\xi p| \leq \sigma^{-1}|\eta q|$. Hence, the perpendicular distance from η to the line pq is larger than $|\xi p|$.
- P5 If auxiliary points η_1, η_2 and η_3 are centered on q and $|q \eta_1| = |q \eta_2|$, then $|q \eta_1| \leq \sigma^{-1}|q \eta_3|$, $\angle \eta_2 q \eta_3 = (\theta/2 - 2\gamma)$, and $\angle q \eta_3 \eta_2 < \gamma$.

Proof. [P1] Note that the largest κ is at most n since there are at most n pairs in the tree. The maximum length between the auxiliary point and its center is at most $\sigma^n \chi^{-1} = d_0^{-1} \Delta$.

[P2] Note that each point $q \in \mathcal{P}_m^n$ belongs to at most three gadgets, one pair ϕ such that $q \in G_\phi$ and two sibling pairs φ_1 and φ_2 such that $q \in \varphi_1 \cap \varphi_2$. See Figure 25 for an example. We visit ϕ first and then φ_1 and φ_2 in order. Note that q is the shared point of φ_1 and φ_2 . According to the way to add auxiliary point, when we visit φ_2 , q corresponds to the point “ w_1 ” (in Figure 24) in

the rules. Thus, we do not add auxiliary points for q . Hence, there are only two times that q can become a center for auxiliary points. The first time happens when we visit ϕ and the second time happens when we visit φ_1 .

[P3] Followed by the proof of [P2], in the first time, we add two auxiliary points η_1 and η_2 centered on q . In the second time, we add one auxiliary point η_3 centered on q . Thus, there are at most three auxiliary points centered on a normal point.

[P4] Suppose p belongs to subtree \mathcal{T}_φ and q belongs to subtree \mathcal{T}_ϕ and $\varphi \prec \phi$. Thus, the auxiliary points are added for p earlier than q . It means that $|\xi p| \leq \sigma^{-1}|\eta q|$. Note that the acute angle between ηq and pq is $(\theta/2 - \gamma)$ and $\sigma > \sin^{-1}(\theta/2 - \gamma)$. Thus, the perpendicular distance from η to the line pq is larger than $|\xi p|$. See Figure 26.

[P5] According to the proof of [P3] (see Figure 25) we add η_1 and η_2 earlier than η_3 . According to the construction, we can add these three auxiliary points for q . Checking the four cases in construction, we can get $\angle(pq, q\eta_3) = -\gamma$ and $\angle(pq, q\eta_2) = -\theta/2 + \gamma$. Thus, $\angle\eta_2 q \eta_3 = \theta/2 - 2\gamma$. Moreover, note that $\sigma > \sin(\theta/2 - \gamma)/\sin \gamma$ and $|\eta_2 q| < \sigma^{-1}|\eta_3 q|$. According to the law of sines, we get $\angle q \eta_3 \eta_2 < \gamma$. \square

Extended hinge set: We extend the concept of hinge sets to the *extended hinge set* to include auxiliary points. The extended hinge set consists of the normal points in the hinge set and the auxiliary points centered on these normal points. Besides, if p belongs to \mathcal{T}_ϕ , then the auxiliary points centered on p belong to *extended* \mathcal{T}_ϕ . Then Claim 17 is still true for $\mathbb{Y}\mathbb{Y}_{2k+1}(\mathcal{P}_m)$ with the same proof. It means that we only need to consider the long range connections between the descendants of any two sibling pairs.

Moreover, we can get similar properties as Lemma 19 and 20 for the auxiliary points. Suppose ϕ and φ are two sibling pairs. If $p \in \mathcal{T}_\phi$ and $q \in \mathcal{T}_\varphi$ and there is a long range connection \vec{pq} in $\mathbb{Y}\mathbb{Y}_{2k+1}$, then $\phi \prec \varphi$. Meanwhile, the points in \mathcal{T}_φ locate in two cones of p . But only one of the two cones may contain a long range connection. We describe the property formally as follows.

Lemma 25. Given a pair (v_1, v_2) at *level*- l for $l < m - 1$, with child-pair set Φ , consider two sibling pairs ϕ and φ in Φ where $\phi = (w_1, w_2)$. p is a point in extended \mathcal{T}_ϕ and q is a point in extended \mathcal{T}_φ . Suppose there is a directed edge \vec{pq} in $\mathbb{Y}\mathbb{Y}_{2k+1}(\mathcal{P}_m)$.

- If $\angle(v_1 v_2, w_2 w_1) = \theta/2$, then $\angle(v_1 v_2, pq) \in (-\theta, 0]$.
- If $\angle(v_1 v_2, w_2 w_1) = -\theta/2$, then $\angle(v_1 v_2, pq) \in (0, \theta]$.

Proof. The proof follows the same procedure as the proof of Lemma 19 and 20. We also distinguish into two cases. Given a pair (v_1, v_2) and its child-pair set Φ , consider two sibling pairs ϕ and φ in Φ where $\phi = (w_1, w_2)$. The first case is that $\angle(v_1 v_2, w_2 w_1) = \theta/2$. The second case is that $\angle(v_1 v_2, w_2 w_1) = -\theta/2$. Consider a point p in extended \mathcal{T}_ϕ . p can be a normal point or an auxiliary point.

Consider that $\angle(v_1 v_2, w_2 w_1) = \theta/2$. First, suppose w_1 is the partition point and ϕ is on the right side of $\vec{v_1 v_2}$. See Figure 27a. Suppose q belongs to \mathcal{T}_φ and $\varphi \prec \phi$ (i.e., $q = q^{(1)}$ in Figure 27a). Denote the partition point in \mathcal{A}_ϕ closest to w_2 by ξ . Because of the projection of points in \mathcal{T}_φ , ξ has two auxiliary points, denoted by ξ_1 and ξ_2 . Thus, \vec{pq} is not an edge in the Yao-step since ξ_1 and q are in the same cone of p . Then consider that q belongs to \mathcal{T}_φ and $\varphi \succ \phi$ (i.e., $q = q^{(2)}$ in Figure 27a). Denote the point in \mathcal{B}_ϕ closest to w_1 by η . According to the fact that $w_1 \eta$ is the

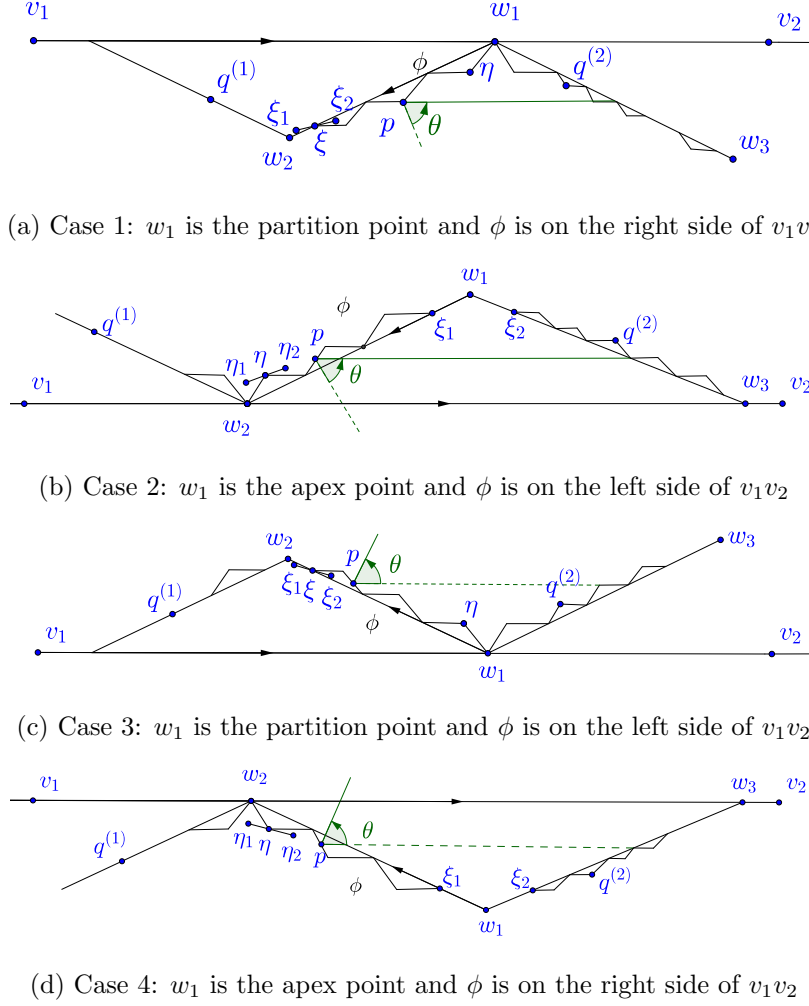


Figure 27: Here $\phi = (w_1, w_2)$ and p belongs to the extended \mathcal{T}_ϕ which includes auxiliary points.

maximum length pair among the child-pairs of ϕ (see Corollary 13), η and q are in the same cone of p when $\angle(v_1v_2, pq) > 0$. Thus, there is no long range connection for p in cone $C_p(0, \theta]$.

Second, suppose w_1 is the apex point and ϕ is on the left side of $\overrightarrow{v_1v_2}$. See Figure 27b. Denote the closest point in \mathcal{B}_ϕ to w_2 by η . Suppose q belongs to \mathcal{T}_ϕ and $\varphi \prec \phi$ (i.e., $q = q^{(1)}$ in Figure 27b). Because of the projection of points in \mathcal{T}_ϕ , η has two auxiliary points, denoted by η_1 and η_2 . There is no edge \overrightarrow{pq} in the Yao-step since η_1 and q are in the same cone p and $|\eta_1p| < |qp|$. Then consider that q belongs to \mathcal{T}_ϕ and $\varphi \succ \phi$ (i.e., $q = q^{(2)}$ in Figure 27b). If q in the cone $C_p(0, \theta]$, q and w_1 are in the same cone of p and $|pw_1| < |pq|$. Thus, in the Yao-step, there is no edge from p to q in the cone $C_p(0, \theta]$. Thus, we prove the first part of the lemma.

Next, we consider the case $\angle(v_1v_2, w_2w_1) = -\theta/2$. First, we consider the case in which w_1 is the partition point and ϕ is on the left side of $\overrightarrow{v_1v_2}$. See Figure 27c. Denote the partition point in \mathcal{A}_ϕ closest to w_2 by ξ . According to the construction for auxiliary point (case 2a), we add two auxiliary points ξ_1 and ξ_2 such that $|\xi\xi_1| = |\xi\xi_2| = \sigma^\kappa\chi^{-1} + \epsilon_0$. If q is in \mathcal{T}_ϕ and $\varphi \prec \phi$ (i.e., $q = q^{(1)}$ in Figure 27c), ξ_1 and q are in the same cone of p . Because the distance $|\xi\xi_1|$ ($> \sigma^\kappa\chi^{-1}$) is slightly

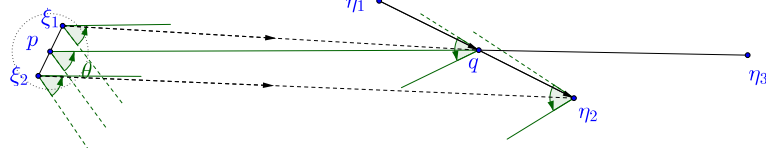


Figure 28: The case that $q \in \mathcal{A}_\phi \cup \mathcal{B}_\phi$. The figure is an enlarged view of Figure 25. q may have three auxiliary points $\{\eta_1, \eta_2, \eta_3\}$. ξ_1 and ξ_2 are two possible positions of the auxiliary point ξ centered on p .

longer than the distances from other auxiliary points of \mathcal{G}_ϕ to their centers. Thus, \vec{pq} is not an edge in the Yao-step since $|\xi_1 p| < |pq|$ and ξ_1 and q are in the same cone of p . Then consider that q (i.e., $q = q^{(2)}$) in Figure 27c) is in \mathcal{T}_φ and $\varphi \succ \phi$. If $\angle(v_1 v_2, pq) \in [-\theta/2, 0]$, \vec{pq} is not a directed edge in Yao-step since w_1 and q are in the same cone and $|w_1 p| < |pq|$.

Finally, we consider the case that w_1 is the apex point and ϕ is on the right side of $\overrightarrow{v_1 v_2}$. Suppose η is the apex point in \mathcal{B}_ϕ closest to w_2 . η_1 and η_2 are auxiliary points of η . If q is in \mathcal{T}_φ and $\varphi \prec \phi$ (i.e., $q = q^{(1)}$ in Figure 27d), η_1 and q are in the same cone of p according to the construction for auxiliary point (case 2b). Thus, \vec{pq} is not an edge in the Yao-step since $|p\eta_1| < |pq|$. Then consider q is in \mathcal{T}_φ and $\varphi \succ \phi$ (i.e., $q = q^{(2)}$ in Figure 27d). If the polar angle of pq belongs to $(-\theta, 0]$, w_1 and q are in the same cone. Thus, there is no edge from p to q since $|pq| > |pw_1|$. Thus, we prove the second part of the lemma.

Overall, we have proved the lemma. \square

Then, we prove that after adding the auxiliary points, there is no long range connection.

Lemma 26. There is no long range connection in $\mathcal{YY}_{2k+1}(\mathcal{P}_m)$.

Proof. Consider a pair (v_1, v_2) and the set Φ of its child-pairs. Suppose $\phi, \varphi \in \Phi$ and $\varphi \prec \phi$. p is a point in \mathcal{T}_φ . Denote an auxiliary point centered on p , if any, by ξ . Let $u \in \{p, \xi\}$. There exists a point q closest to p such that $q \in \mathcal{T}_\phi$ and pq is parallel to $v_1 v_2$ based on the projection process. If not, i.e., \mathcal{T}_ϕ only locates in one cone of p , according to Lemma 25, there is no long range connection between u and points in extended \mathcal{T}_ϕ .

According to Lemma 25, first, there is no directed edge from a point in (extended) \mathcal{T}_ϕ to (extended) \mathcal{T}_φ . Next, we prove there is no long range connection from \mathcal{T}_φ to \mathcal{T}_ϕ . Since p is an arbitrary point in \mathcal{T}_φ , we prove that there is no long range connection between u and the points in \mathcal{T}_ϕ , (recall $u \in \{p, \xi\}$). According to whether q is in $\mathcal{A}_\phi \cup \mathcal{B}_\phi$ or ϕ , there are two cases.

q belongs to $\mathcal{A}_\phi \cup \mathcal{B}_\phi$: q has two auxiliary points η_1 and η_2 because of the projection \vec{pq} and q is a candidate center. Note that q may have a third auxiliary point η_3 . But p and η_3 are on the two different sides of $\eta_1 \eta_2$ and $|\eta_3 q| > |\eta_1 q| = |\eta_2 q|$ because of Property 24[P5]. Therefore, there is no directed edge $p\eta_3$ in the Yao-step because η_2 and η_3 are in the same cone of p and $|\eta_2 p| < |\eta_3 p|$. According to Property 24[P4], $|\xi p|$ is much less than $|\eta_1 q|$ or $|\eta_2 q|$ and the perpendicular distance from η_1 and η_2 to the line pq is longer than $|\xi p|$. Suppose $u \in \{p, \xi\}$. See Figure 28 which is an enlarged view of Figure 25, in which ξ_1 and ξ_2 are two possible positions of ξ . According to Lemma 25, $u\eta_1$ does not exist in the Yao-step since η_1 and one point of ϕ (denoted by w_1 , refer to Figure 25) are in the same cone of u and $|w_1 u| < |\eta_1 u|$. If there is an edge $u\eta_2$ in the Yao-step, the edge $u\eta_2$ cannot be accepted by η_2 in the reverse-Yao step since $q\eta_2$ exists, and point q and u are

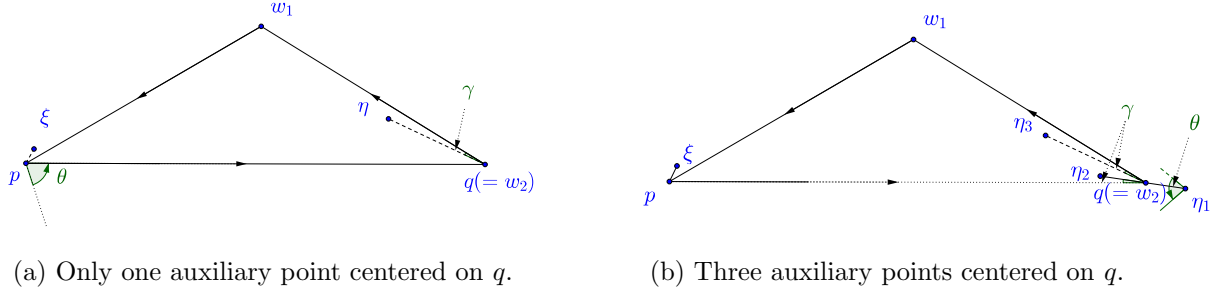


Figure 29: q is a point of pair ϕ , i.e., $q = w_2$.

in the same cone of q and $|q\eta_2| < |u\eta_2|$. If there is an edge uq in the Yao-step, the edge uq cannot be accepted by q in the reverse-Yao step since η_1 and u are in the same cone and $|\eta_1q| < |uq|$. Therefore, there is no long range connection related to p and its auxiliary points.

q belongs to ϕ : See Figure 29. Note that in this case, q is point w_2 of ϕ . According to Property 24[P3], any point has at most three auxiliary points. Since q is a projection point of p , q has at least one auxiliary point. Thus, there are two possible situations. One is that there is only one auxiliary point centered on q (see Figure 29a). It means that in the first time that q was able to be a candidate center, there is no auxiliary point added centered on it (see the proof of Property 24[P2]). Denote the auxiliary point of q by η . Let $u \in \{p, \xi\}$ where ξ is an auxiliary point centered on p . According to the Property 24[P4], η and w_1 are in the same cone of u and $|uw_1| < |u\eta|$. Therefore, there is no edge $u\eta$ in the Yao-step. Moreover, uq cannot be accepted in the reverse-Yao step. Because the edge ηq exists in the Yao-step. u and η are in the same cone of q and $|\eta q| < |uq|$. Combining with Lemma 25, there is no long range connection from u to \mathcal{T}_ϕ . The second case is that there are three auxiliary points of q (see Figure 29b). Denote the auxiliary points of q by $\{\eta_1, \eta_2, \eta_3\}$. According to Property 24[P5], we know $\angle \eta_2 q \eta_3 = (\theta/2 - 2\gamma)$. Again, denote $u \in \{p, \xi\}$. There is no edge $u\eta_3$ in the Yao-step since w_1 and η_3 are in the same cone of u and $|uw_1| < |u\eta_3|$. There is no edge $u\eta_1$ in the reverse-Yao step, since there is an edge $q\eta_1$ in the Yao-step and $|q\eta_1| < |u\eta_1|$. Similarly, there is no edge uq since there is an edge $\eta_2 q$ in the Yao-step and $|\eta_2 q| < |uq|$. Next, note that $|q\eta_2| \leq \sigma^{-1}|q\eta_3|$. According to Property 24[P5], we know η_3 and u are in the same cone of η_2 . Thus, there is no edge from $u\eta_2$.

Overall, we prove that there is no long range connection in $\mathbb{Y}\mathbb{Y}_{2k+1}(\mathcal{P}_m)$. \square

6 The Length Between μ_1 and μ_2 in $\mathbb{Y}\mathbb{Y}_{2k+1}(\mathcal{P}_m)$

In this section, we prove that the length of the shortest path between the initial points μ_1 and μ_2 in $\mathbb{Y}\mathbb{Y}_{2k+1}(\mathcal{P}_m)$ diverges as m approaches infinity.

First, recall that we have extended the concept of hinge sets to *extended hinge sets* which consist of the normal points in the hinge set and the auxiliary points of these normal points. Consider two extended hinge sets Λ and Λ' . Define the shortest path between Λ and Λ' to be the shortest path in $\mathbb{Y}\mathbb{Y}_{2k+1}(\mathcal{P}_m)$ between any two points p and q such that $p \in \Lambda$ and $q \in \Lambda'$. Consider any pair $\phi = (w_1, w_2)$ at level- $(m-1)$. We give a lower bound on the shortest path distance between its former extended hinge set and latter extended hinge set.

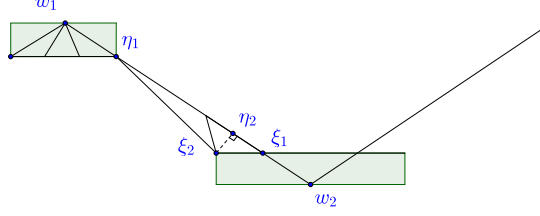


Figure 30: The shortest Euclidean distance between two hinge sets centered on points of a pair $\phi = (w_1, w_2)$ at $level-(m-1)$.

Lemma 27. Consider any pair (w_1, w_2) at $level-(m-1)$. Denote its former extended hinge set by $\Lambda_\phi^{(-)}$, and latter extended hinge set by $\Lambda_\phi^{(+)}$. The shortest path distance between $\Lambda_\phi^{(-)}$ and $\Lambda_\phi^{(+)}$ is at least $(1 - 6d_0^{-1})|w_1w_2|$.

Proof. Let $|w_1w_2| = \delta$. See Figure 30. Note that $\Lambda_\phi^{(-)}$ and $\Lambda_\phi^{(+)}$ (the two hinge sets centered on w_1 and w_2) are not overlapping. Denote the near-empty piece incident on w_1 by $w_1\eta_1$ and the empty piece incident on w_2 by $w_2\xi_1$. $\xi_1\xi_2$ is the leaf-pair closest to w_2 . $\xi_2\eta_2$ is perpendicular to w_1w_2 . The shortest Euclidean distance between the two hinge sets is no less than $|\eta_1\eta_2|$. According to Property 14, $|w_1\eta_1| \leq 2d_0^{-1}\delta$, $|w_2\xi_1| \leq d_0^{-1}\delta$ and $\xi_1\eta_2 \leq 0.5d_0^{-1}\delta$. Thus, $|\eta_1\eta_2| > (1 - 3.5d_0^{-1})\delta$.

Then consider the auxiliary points. Note that according to the Property 24[P1], the maximum distance between an auxiliary point and its center is $d_0^{-1}\Delta$, where Δ is the minimum distance between any two normal points. Since $\Delta \leq \delta$, according to triangle inequality, the auxiliary points can reduce the distance between the two hinge sets by at most $2d_0^{-1}\delta$. Overall, the shortest path between $\Lambda_\phi^{(-)}$ and $\Lambda_\phi^{(+)}$ is at least $(1 - 6d_0^{-1})|w_1w_2|$. \square

According to Lemma 26, there is no long range connection in $\mathbb{Y}\mathbb{Y}_{2k+1}(\mathcal{P}_m)$. Thus, the shortest path between μ_1 and μ_2 should pass through all hinge sets in order. Thus, for each pair ϕ at $level-(m-1)$, there is a path between $\Lambda_\phi^{(-)}$ and $\Lambda_\phi^{(+)}$.

Let the shortest path between $\Lambda_\phi^{(-)}$ and $\Lambda_\phi^{(+)}$ be Δ_ϕ . Then, we prove that the sum of lengths of Δ_ϕ over all pairs at $level-(m-1)$ diverges as m approaches infinity. Thus, the length of the shortest path between μ_1 and μ_2 diverges too.

Lemma 28. The length of the shortest path between μ_1 and μ_2 in $\mathbb{Y}\mathbb{Y}_{2k+1}(\mathcal{P}_m)$ for $k \geq 3$ is at least ρ^m , for some $\rho = (1 - O(d_0^{-1})) \cdot \cos^{-1}(\theta/2)$. Thus, by setting $d_0 > \lceil 6(1 - \cos(\theta/2))^{-1} \rceil$, the length diverges as m approaches infinity.

Proof. We give a lower bound of the sum of lengths $|w_1w_2|$ over all pairs (w_1, w_2) at $level-(m-1)$. Recall that the length of a pair is the length of the segment between the two points of the pair. Consider any pair $\phi = (v_1, v_2)$ with length δ . According to Property 14, the sum of lengths of half-empty, near-empty and empty pieces is no more than $6d_0^{-1}\delta$. Thus, the pieces which generate internal-pairs in next level have length at least $(1 - 6d_0^{-1})\delta$. For each piece, it generates two child-pairs. The sum of lengths of the two pairs is $\cos^{-1}(\theta/2)$ times larger than the piece itself. Overall, the sum of the lengths of the pairs in generated next levels is at least $(1 - 6d_0^{-1})\delta \cos^{-1}(\theta/2)$. Let $\rho = (1 - 6d_0^{-1}) \cos^{-1}(\theta/2)$. Thus, after $(m-1)$ rounds, the length of the pairs at $level-(m-1)$

is at least $\rho^{m-1}|\mu_1\mu_2|$. According to Lemma 27, the shortest path from μ_1 to μ_2 is at least $(1 - 6d_0^{-1})\rho^{m-1}|\mu_1\mu_2|$. When $d_0 > 6(1 - \cos(\theta/2))^{-1}$, the shortest path between μ_1 and μ_2 in $\mathsf{YY}_{2k+1}(\mathcal{P}_m)$ diverges as m approaches infinity. \square

Finally, combining with the results that YY_3 [15] and YY_5 [2] may not be spanners, we have proved Theorem 4.

Theorem 4 (restated). *For any $k \geq 1$, there exists a class of instances $\{\mathcal{P}_m\}_{m \in \mathbb{Z}^+}$ such that the stretch factor of $\mathsf{YY}_{2k+1}(\mathcal{P}_m)$ cannot be bounded by any constant, as m approaches infinity.*

References

- [1] Franz Aurenhammer. Voronoi diagrams – survey of a fundamental geometric data structure. *ACM Computing Surveys (CSUR)*, 23(3):345–405, 1991.
- [2] Luis Barba, Prosenjit Bose, Mirela Damian, Rolf Fagerberg, Wah Loon Keng, Joseph O’Rourke, André van Renssen, Perouz Taslakian, Sander Verdonschot, and Ge Xia. New and improved spanning ratios for Yao graphs. *JoCG*, 6(2):19–53, 2015.
- [3] Luis Barba, Prosenjit Bose, Jean-Lou De Carufel, André van Renssen, and Sander Verdonschot. On the stretch factor of the Θ_4 -graph. In *Workshop on Algorithms and Data Structures*, pages 109–120. Springer, 2013.
- [4] Matthew Bauer and Mirela Damian. An infinite class of sparse-Yao spanners. In *Proceedings of the Twenty-Fourth Annual ACM-SIAM Symposium on Discrete Algorithms*, pages 184–196. SIAM, 2013.
- [5] Nicolas Bonichon, Cyril Gavoille, Nicolas Hanusse, and David Ilcinkas. Connections between Θ -graphs, Delaunay triangulations, and orthogonal surfaces. In *International Workshop on Graph-Theoretic Concepts in Computer Science*, pages 266–278. Springer, 2010.
- [6] Prosenjit Bose, Mirela Damian, Karim Douïeb, Joseph O’rourke, Ben Seamone, Michiel Smid, and Stefanie Wührer. $\pi/2$ -angle Yao graphs are spanners. *International Journal of Computational Geometry & Applications*, 22(01):61–82, 2012.
- [7] Prosenjit Bose, Anil Maheshwari, Giri Narasimhan, Michiel Smid, and Norbert Zeh. Approximating geometric bottleneck shortest paths. *Computational Geometry*, 29(3):233–249, 2004.
- [8] Prosenjit Bose, Pat Morin, André van Renssen, and Sander Verdonschot. The Θ_5 -graph is a spanner. *Computational Geometry*, 48(2):108–119, 2015.
- [9] Prosenjit Bose, André van Renssen, and Sander Verdonschot. On the spanning ratio of theta-graphs. In *Workshop on Algorithms and Data Structures*, pages 182–194. Springer, 2013.
- [10] Paul Chew. There is a planar graph almost as good as the complete graph. In *Proceedings of the second annual symposium on Computational geometry*, pages 169–177. ACM, 1986.
- [11] Mirela Damian. A simple Yao-Yao-based spanner of bounded degree. *arXiv preprint arXiv:0802.4325*, 2008.
- [12] Mirela Damian, Nawar Molla, and Val Pinciu. Spanner properties of $\pi/2$ -angle Yao graphs. In *Proc. of the 25th European Workshop on Computational Geometry*, pages 21–24. Citeseer, 2009.
- [13] Mirela Damian and Naresh Nelavalli. Improved bounds on the stretch factor of Y_4 . *Computational Geometry*, 62:14–24, 2017.
- [14] Mirela Damian and Kristin Raudonis. Yao graphs span Θ -graphs. In *Combinatorial Optimization and Applications*, pages 181–194. Springer, 2010.

- [15] Nawar M El Molla. Yao spanners for wireless ad hoc networks. Master’s thesis, Villanova University, 2009.
- [16] David Eppstein. Spanning trees and spanners. *Handbook of computational geometry*, pages 425–461, 1999.
- [17] David Eppstein. Beta-skeletons have unbounded dilation. *Computational Geometry*, 23(1):43–52, 2002.
- [18] BE Flinchbaugh and LK Jones. Strong connectivity in directional nearest-neighbor graphs. *SIAM Journal on Algebraic Discrete Methods*, 2(4):461–463, 1981.
- [19] K Ruben Gabriel and Robert R Sokal. A new statistical approach to geographic variation analysis. *Systematic Biology*, 18(3):259–278, 1969.
- [20] Matthias Grünewald, Tamás Lukovszki, Christian Schindelhauer, and Klaus Volbert. Distributed maintenance of resource efficient wireless network topologies. In *European Conference on Parallel Processing*, pages 935–946. Springer, 2002.
- [21] Lujun Jia, Rajmohan Rajaraman, and Christian Scheideler. On local algorithms for topology control and routing in ad hoc networks. In *Proceedings of the fifteenth annual ACM symposium on Parallel algorithms and architectures*, pages 220–229. ACM, 2003.
- [22] Iyad A Kanj and Ge Xia. On certain geometric properties of the Yao-Yao graphs. In *Combinatorial Optimization and Applications*, pages 223–233. Springer, 2012.
- [23] Jian Li and Wei Zhan. Almost all even Yao-Yao graphs are spanners. *The 24rd Annual European Symposium on Algorithms*, 2016.
- [24] Xiang-Yang Li. *Wireless Ad Hoc and Sensor Networks: Theory and Applications*. Cambridge, 6 2008.
- [25] Xiang-Yang Li, Peng-Jun Wan, and Yu Wang. Power efficient and sparse spanner for wireless ad hoc networks. In *Computer Communications and Networks, 2001. Proceedings. Tenth International Conference on*, pages 564–567. IEEE, 2001.
- [26] Xiang-Yang Li, Peng-Jun Wan, Yu Wang, and Ophir Frieder. Sparse power efficient topology for wireless networks. In *System Sciences, 2002. HICSS. Proceedings of the 35th Annual Hawaii International Conference on*, pages 3839–3848. IEEE, 2002.
- [27] Giri Narasimhan and Michiel Smid. *Geometric spanner networks*. Cambridge University Press, 2007.
- [28] Jim Ruppert and Raimund Seidel. Approximating the d -dimensional complete euclidean graph. In *Proceedings of the 3rd Canadian Conference on Computational Geometry (CCCG 1991)*, pages 207–210, 1991.
- [29] Jörg-Rüdiger Sack and Jorge Urrutia. *Handbook of computational geometry*. Elsevier, 1999.
- [30] Christian Schindelhauer, Klaus Volbert, and Martin Ziegler. Spanners, weak spanners, and power spanners for wireless networks. In *International Symposium on Algorithms and Computation*, pages 805–821. Springer, 2004.

- [31] Christian Schindelhauer, Klaus Volbert, and Martin Ziegler. Geometric spanners with applications in wireless networks. *Computational Geometry*, 36(3):197–214, 2007.
- [32] Godfried T Toussaint. The relative neighbourhood graph of a finite planar set. *Pattern recognition*, 12(4):261–268, 1980.
- [33] Yu Wang, Xiang-Yang Li, and Ophir Frieder. Distributed spanners with bounded degree for wireless ad hoc networks. *International Journal of Foundations of Computer Science*, 14(02):183–200, 2003.
- [34] Andrew Chi-Chih Yao. On constructing minimum spanning trees in k -dimensional spaces and related problems. *SIAM Journal on Computing*, 11(4):721–736, 1982.